UNIVERSITY
OF
QUEENSLAND

Department of Civil Engineering

RESEARCH REPORT SERIES

Buckling Approximations For Laterally Continuous Elastic I-Beams

P. F. DUX and
S. KITIPORNCHAI

Research Report No. CE11
April, 1980

CIVIL ENGINEERING RESEARCH REPORTS

This report is one of a continuing series of Research Reports published by the Department of Civil Engineering at the University of Queensland. This Department also publishes a continuing series of Bulletins. Lists of recently published titles in both of these series are provided inside the back cover of this report. Requests for copies of any of these documents should be addressed to the Departmental Secretary.

The interpretations and opinions expressed herein are solely those of the author(s). Considerable care has been taken to ensure the accuracy of the material presented. Nevertheless, responsibility for the use of this material rests with the user.

Department of Civil Engineering,
University of Queensland,
St Lucia, Q 4067, Australia,
[Tel:(07) 377-3342, Telex:UNIVQLD AA40315]

BUCKLING APPROXIMATIONS FOR LATERALLY CONTINUOUS ELASTIC I-BEAMS

by

P. F. Dux, BE, M Eng Sc.
Senior Tutor in Civil Engineering

and

S. Kitipornchai, BE, PhD
Senior Lecturer in Civil Engineering

RESEARCH REPORT NO. CE 11
Department of Civil Engineering
University of Queensland
April, 1980

Synopsis

An approximate method for determining the elastic flexural-torsional buckling loads of laterally continuous structures is developed. The method is a refinement of that proposed by Nethercot and Trahair and can be applied to structures loaded at braced points. The braces and supports are assumed to prevent lateral deflection and twisting. The procedure locates a critical segment and adjacent restraining segments which together form a sub-structure. The elastic critical load is obtained by determining the effective length of the critical segment. Charts of effective length factors, k, are presented and are shown to depend on the end restraint parameters, G_A and G_B, the segment beam parameter, K, and the end moment ratio, β. The proposed method is applied to a number of worked examples. The results are in close agreement with accurate numerical solutions.

The paper has been written with the design engineer in mind and does not presuppose a detailed knowledge of buckling theory.

CONTENTS

1. INTRODUCTION

The ultimate strength of an I-beam having continuous or very closely spaced lateral support is determined by its plastic moment capacity. If insufficient lateral support exists, the beam may fail by flexural-torsional buckling in either the elastic or the inelastic range. In various design codes (5-7) the elastic buckling loads form the basis for determining the design loads of slender beams and of beams with intermediate slenderness. Computer methods and some solutions (8-11) are available for analysing the elastic and inelastic buckling of isolated beams with a variety of support and loading conditions. However, there is a need also for reliable approximate methods which obviate the need for a computer and suitable program. This paper presents such a method for the stability analysis of ideal elastic laterally continuous structures loaded at braced points.

The paper first emphasises some relevant principles of stability of laterally continuous beams. Various assumptions are then made in order to reduce the complexity of behaviour to a level suitable for approximate analysis. The concept of effective length is then used in the development of an approximate method of analysis which is a refinement of that proposed by Nethercot and Trahair (1-4).

2. STRUCTURAL BEHAVIOUR

2.1 Basic Assumptions

Although particular reference is made to beams throughout the paper, the principles and the method are equally applicable to other laterally continuous structures (see Fig. 1). These include braced cantilevers and some simple grids of narrow rectangular beams or of members having section properties or dimensions such that the torsional resistance associated with restraint of warping is relatively insignificant. The basic assumptions are:

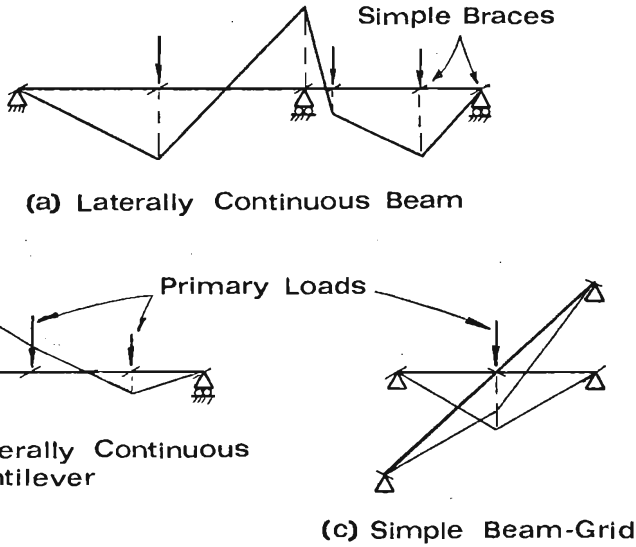

FIGURE 1 : Laterally continuous structures

(i) no out-of-plane deformations occur prior to the structure reaching its buckling load;

(ii) the braces and the supports prevent lateral deflection and twisting of the cross-section;

(iii) the primary loads produce only major axis moment patterns of constant gradient in the various beam segments, and

(iv) no changes in moment patterns occur as loads increase.

2.2 Buckling of a Single Segment

The dimensionless elastic buckling moment γ_c, of a simply supported segment (see Fig. 2) can be expressed in the form,

$$\gamma_c = \frac{M_E L}{\sqrt{EI_y GJ}} = m\pi \sqrt{1+K^2} \qquad (1)$$

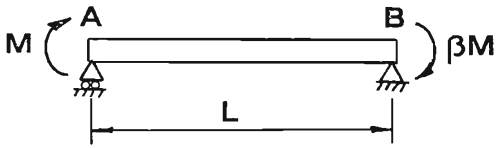

FIGURE 2 : Simply supported segment with end moments

where K is the beam parameter,

$$K = \sqrt{\frac{\pi^2 EI_\omega}{L^2 GJ}} \qquad (2)$$

and EI_y is the minor axis bending rigidity, GJ is the torsional rigidity, EI_ω is the warping rigidity, L is the segment length and m is the moment modification factor which allows for the major axis moment distribution. It is approximated (12) by

$$m = 1.75 + 1.05\beta + 0.3\beta^2 \leq 2.56 \qquad (3)$$

where β, the major axis moment ratio, lies within the range $-1.0 < \beta < 1.0$. A uniform major axis moment corresponds to $\beta = -1.0$ and $m = 1.0$.

The beam parameter, K, in Equation 2 is a measure of the significance of the torsional resistance developed by the variation of internal warping restraint along the segment when under non-uniform torsion (14). For beams of narrow rectangular cross-section, the value of K is zero.

In Fig. 2 and throughout the paper, the larger major axis end moment, M, occurs at end A of the segment. In simply supported segments, M has a limiting value of M_E as defined in Equation 1.

2.3 Interaction Buckling

As the primary loads on a laterally continuous beam increase, its resistance to a set of disturbing forces tending to produce buckling deformations gradually diminishes. When the loads are sufficiently large, the structure reaches a state of neutral equilibrium and is able to maintain a particular

mode shape without the assistance of disturbing forces. The out-of-plane or disturbing components of primary forces and moments which develop when the beam adopts the mode shape enable it to remain in equilibrium. It is assumed that the beam fails when it has the ability to adopt a mode shape. The post-buckling capacity increase exhibited by some beams is not of interest in this paper.

The existence of mode shapes implies that the whole structure interacts and participates in a single buckling action. The common practice of dissassembling a beam into a number of simply supported segments (13) and estimating beam failure loads from the separate stability analyses of the isolated segments without accounting for interaction may lead to incorrect solutions.

To demonstrate the above point, consider a simply supported narrow rectangular beam (Fig. 3) carrying a uniform major axis moment, M. The beam has simple braces at the supports and at the quarter points. The dimensionless elastic critical moments, γ_c, of the beam assuming

(a) individual segment buckling without interaction; and

(b) buckling interaction

are compared in Table 1.

In Table 1, the dimensionless buckling moments, γ_c, are expressed in terms of L, the beam length. If interaction is neglected a limiting value of 2π is indicated. The result of a more precise analysis (11) allowing for segment interaction shows that the beam fails when $\gamma_c = 2.86\pi$. Segment 2-3 receives restraint from the stockier end ones, and, at beam buckling, has an effective length less than unity whereas the end segments have effective lengths greater than unity.

Apart from demonstrating segment interaction, the example shows that it is not possible for some portion of a structure to restrain another portion without itself being destabilised and hence, the actual buckling moment lies between the individual segment values.

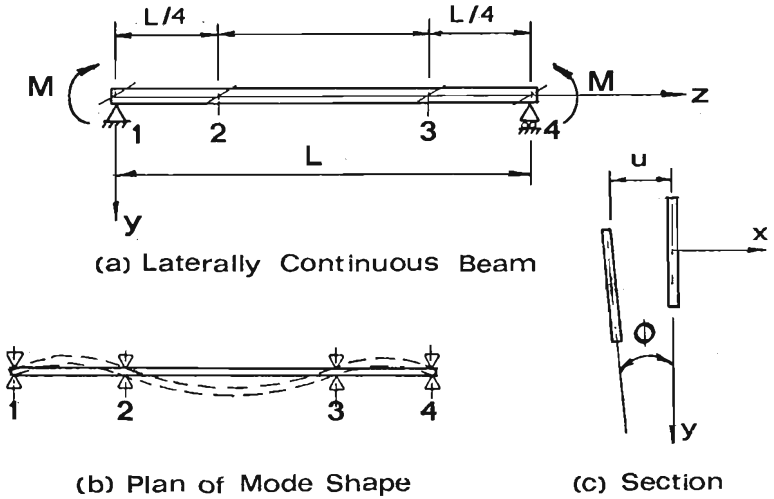

FIGURE 3 : Rectangular beam under uniform moment

TABLE 1

Comparison of Beam Failure Loads

Segment	Dimensionless Buckling Moments, γ_c		Calculated Effective Length Factor, k
	(a) No Interaction	(b) Interaction (11)	
1-2	4π	2.86π	1.4
2-3	2π	2.86π	0.7
3-4	4π	2.86π	1.4

The reciprocal nature of interaction and the approach to instability of some simple beams such as that in Fig. 3 can be illustrated graphically. The following observations are made. Firstly, the behaviour of a narrow rectangular beam free from axial load can be described in terms of major axis bending, minor axis bending and torsion of the St. Venant type since warping is of no significance. This implies that

segment interaction involves only the bending actions as twisting is prevented at the segment ends. Minor axis bending interaction occurs if the structure is disturbed laterally from its assumed initially straight position. Secondly, the major axis moment pattern indicates that at the lowest buckling load, the beam (Fig. 3(b)) is free to adopt a symmetrical mode shape with two internal points of minor axis bending contraflexure. Between braced points, the beam will twist in response to the torsional component of major axis moment which develops when the beam deflects laterally.

At various stages of loading the stiffness of the beam can be measured by applying the disturbing minor axis moments shown in Fig. 4.

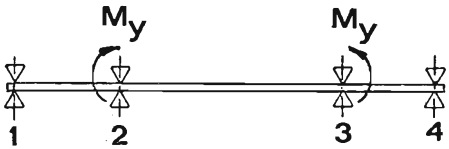

FIGURE 4 : Out-of-plane disturbing moments

The response of the central segment to a uniform minor axis moment and that of the end segments to a single end moment can be expressed in terms of minor axis bending stiffnesses,

$$\frac{M_y}{\theta_y} = f \frac{EI_y}{L_s} \qquad (4)$$

where L_s is the segment length.

The coefficient, f, is a stability function similar to those used in column analysis (15). For the narrow rectangular beam in Figs. 3 and 4, the expressions for the functions f can be derived by solving directly the differential equations of minor axis bending and torsion (16). For segment 2-3,

$$f = f_1 = \frac{(\gamma/2)\sin(\gamma/2)}{1 - \cos(\gamma/2)} \tag{5}$$

and for segments 1-2 and 3-4

$$f = f_2 = \frac{(\gamma/4)^2}{1 - (\gamma/4)\cot(\gamma/4)} \tag{6}$$

where γ is the dimensionless applied major axis moment,

$$\gamma = \frac{ML}{\sqrt{EI_y GJ}} \tag{7}$$

It may be noted that a direct solution is not possible for beams carrying other than a uniform major axis moment. The functions, f_1 and f_2, are plotted in Fig. 5 which also shows the coexisting major axis and minor axis segment moments.

The functions f_1 and f_2 begin with the usual values of 2 and 3 when the major axis moment is zero. As load is applied the functions reduce but the structure remains stable as long as the total stiffnesses at braces 2 and 3 are positive. In the early stages of loading ($\gamma < 2\pi$) all segments have positive stiffness. When γ exceeds 2π, the central segment contributes negative stiffnesses but while γ is less than 2.86π, the end segments have enough reserve of positive stiffness to restrain the weaker one and to resist disburbing forces of the type shown in Fig. 4. Although the central segment is loaded beyond its simply-supported capacity, a finite set of such forces is required to produce buckling deformations and the beam reverts to its original geometry on their removal. As the major axis load increases so does the demand for restraint and the difficulty of the restraining segments to provide it. Eventually the total stiffness is zero and the structure is unable to resist even infinitesimally small disturbing forces. This occurs at a γ value of 2.86π when f_1 is equal to $-2f_2$ (see Fig. 5).

The curves in Fig. 5 indicate that although the whole structure is affected by primary loading, certain parts may

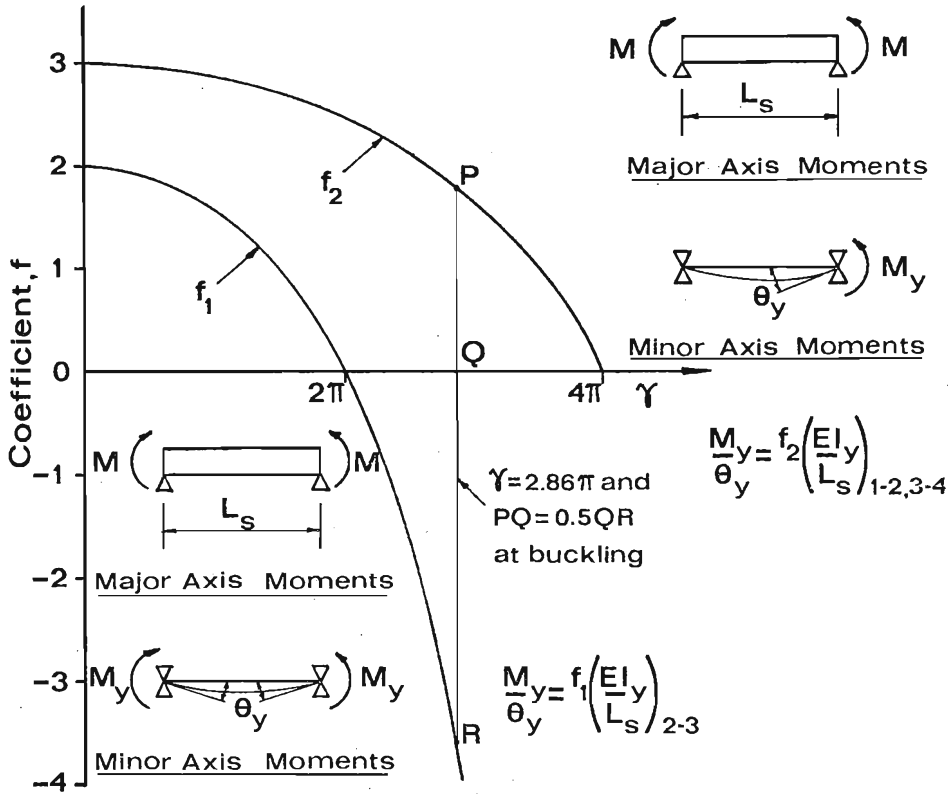

FIGURE 5 : Minor axis bending stiffness

dominate in limiting the capacity. The rate of minor axis bending stiffness degeneration of the central segment increasingly exceeds that of the end segments. Nethercot and Trahair (1-3) have introduced the term "*critical segment*" which in this instance is the central one. The critical segment is found by calculating γ_c from Equation 1 for each segment, and the load factor for the beam necessary to produce γ_c. The critical segment gives the lowest load factor. In References 1-3 and in this paper, the approximate methods are based on the assumption that conditions in the critical segment have a pronounced effect on beam stability.

3. DIRECT STIFFNESS STABILITY ANALYSIS

Usually it is not possible to analyse a general laterally continuous beam by the above procedure using stiffness variation curves. Designers may not have correct knowledge of the mode shape and may choose to apply a set of disturbing forces not necessarily associated with the lowest mode. As well, in most practical I-beams, segment interaction involves not only minor axis bending but also warping actions. This implies that a disturbing force set should have both a minor axis bending moment and a bimoment at each segment end. The generalised displacements or degrees of freedom are a minor axis roation as seen before and a first derivative, with respect to length, of the angle of twist (17). Hence, for a beam with several braces there are many stiffness variation curves from which to interpret interaction. These more complex structures may defy graphical solution but can be studied with several approaches one of which is based on the direct stiffness method of analysis (15).

In the method the structure is modelled as elements and nodes. For the purposes of this paper, the segments can be taken as elements and the supports and braced points as nodes. It is possible to develop a primary load dependent structure stiffness matrix relating a general disturbing nodal force set containing a moment and a bimoment at each node to the set of nodal displacements produced by the forces. Each segment contributes a 4x4 sub-matrix which can be obtained from the numerical solution of the differential equations of minor axis bending and torsion (16). The stiffness relationship summarising the behaviour of the whole structure is written as

$$[R] = [K][r] \qquad (8)$$

that is,

$$\begin{bmatrix}\text{Disturbing}\\ \text{Nodal}\\ \text{Forces}\end{bmatrix} = \begin{bmatrix}\text{Primary Load}\\ \text{Dependent Structure}\\ \text{Stiffness Matrix}\end{bmatrix} \begin{bmatrix}\text{Nodal}\\ \text{Buckling}\\ \text{Displacements}\end{bmatrix}$$

It has been shown in the preceding section that with increasing primary loads, the resistance of the structure to disturbing forces reduces. As the buckling load is closely approached an infinitesimally small set of such forces can produce real buckling displacements provided they tend to produce the correct mode shape. In the limit, the disturbing force set in Equation 8 approaches a null vector although the corresponding nodal displacements are non-trivial. At this stage of primary loading the structure is in neutral equilibrium. For the now homogeneous equations (Equation 8) to have a non-trivial solution the determinant of the coefficient matrix must be zero (18). Each time the determinant of the load dependent stiffness matrix is zero, the primary loads are at a buckling level (15). In particular, the first zero corresponds to the lowest buckling mode. Therefore, by repeatedly altering the primary load factor and observing the value of the determinant, one can perform a stability analysis without having to assume a particular non-trivial disturbing force pattern.

A simply-supported I-beam segment, AB, under major axis end moments M, βM is shown in Fig. 2. At a given moment level, M, the segment stiffness matrix is found by applying the end loads in Fig. 6.

The minor axis moments M_{yA}, M_{yB} and the bimoments B_{MA}, B_{MB} are applied in turn at the segment ends. The boundary conditions $\Theta_y = 0$ and $\phi' = 0$ impose minor axis rotational and warping fixities respectively. Reactive moments and bimoments are developed by these fixities.

The bimoment, B_M, is the generalised force associated with restraint of warping. If the free warping displacements (see Fig. 7(a)) of an I-beam section are partially or fully restrained, longitudinal strains and stresses develop in the flange planes. For I-sections it is convenient to visualise (17) the biomoment as a pair of equal and opposite flange moments, M_f, producing differential flange bending (see Fig. 7(b)). The moments have magnitude B_M/h where h is the distance between flange centroids. The torsional resistance developed by differential warping restraint is measured by the first

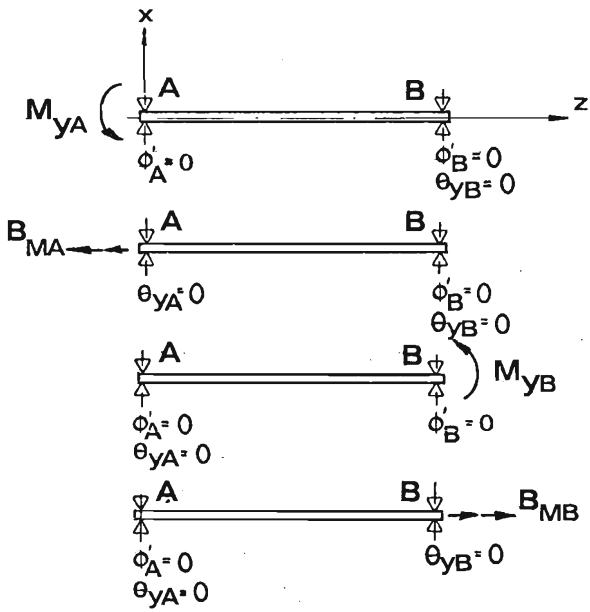

FIGURE 6 : Segment end loads and fixities

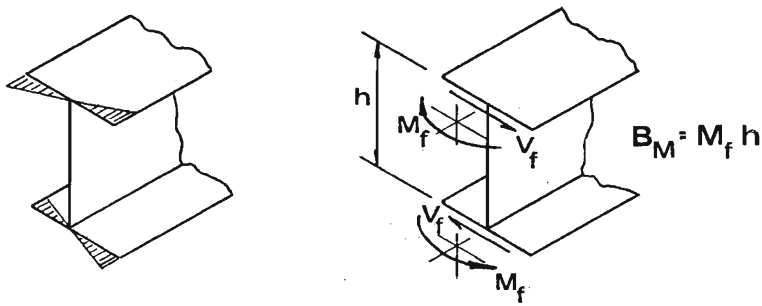

FIGURE 7 : Warping and flange moments in an I-section

derivative, with respect to length, of the bimoment and is equal to the couple produced by flange shears, V_f (= dM_f/dz).

The structure stiffness matrix in Equation 8 is established by assembling all of the segment stiffness matrices. The approximate method which will now be developed focusses on the stiffness matrix of the critical segment alone.

4. APPROXIMATE ANALYSIS

4.1 Substructure and Critical Segment Stiffness Matrix

The critical segment of a laterally continuous beam was defined in Section 2 as that which indicates the lowest beam load factor in an analysis neglecting segment interaction. It was suggested that, when segment interaction is considered, the excessive deterioration of stiffness in this segment and the consequent high levels of restraint demand placed on other segements leads to the eventual collapse of the beam. If this is accepted, a first estimate of the available restraint can be made by examining conditions in the immediately adjacent segments. In this way a substructure comprising the critical setment and the two (at most) adjacent or restraining segments is defined. It is assumed that the behaviour of the substructure adequately reflects the behaviour of the beam. A beam and a typical substructure are shown in Fig. 8.

To fully define the subassemblage, boundary conditions must be imposed at the far ends of the adjacent segments. Support conditions such as the pinned or simply supported end (at brace 6) in Fig. 8 are retained. If the far end of the restraining segment connects to yet another, for example at 3, it is assumed that a restraint demand equal to that of the critical segment is placed at this end. In some instances alternative boundary conditions may be required (see Section 5).

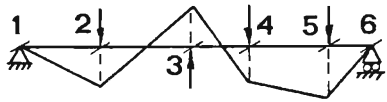

(a) Laterally Continuous Beam

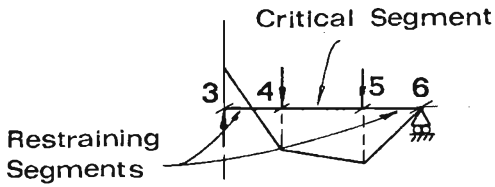

(b) Substructure

FIGURE 8 : Laterally continuous beam and substructure

The stiffness equation of a simply supported critical segment can be written as

$$\begin{bmatrix} \bar{M}_{yA} \\ \bar{B}_{MA} \\ \bar{M}_{yB} \\ \bar{B}_{MB} \end{bmatrix} = \begin{bmatrix} S_{11} & S_{12} & S_{13} & S_{14} \\ S_{21} & S_{22} & S_{23} & S_{24} \\ S_{31} & S_{32} & S_{33} & S_{34} \\ S_{41} & S_{42} & S_{43} & S_{44} \end{bmatrix} \begin{bmatrix} \bar{\Theta}_{yA} \\ \bar{\Theta}'_{A} \\ \bar{\Theta}_{yB} \\ \bar{\Theta}'_{B} \end{bmatrix} \qquad (9)$$

where

$$\left.\begin{aligned} \bar{M}_y &= \frac{M_y L}{\gamma\sqrt{EI_y}} \quad ; \quad \bar{\Theta}_y = \frac{\Theta_y\sqrt{EI_y}}{\gamma} \quad ; \\ \bar{B}_M &= \frac{B_M L^2\sqrt{GJ}}{EI_\omega} \quad ; \quad \bar{\phi}' = \phi' L\sqrt{GJ} \quad ; \\ \gamma &= \frac{ML}{\sqrt{EI_y GJ}} \end{aligned}\right\} \qquad (10)$$

The various terms (S_{11} .... S_{44}) are dependent on the ratio of the major axis moment and the elastic buckling moment, M/M_E, the moment gradient, β, and the beam parameter, K. The forces and displacements have been modified so that the stiffness matrix terms are dimensionless stability functions. The lowest load at which the determinant of the stiffness matrix becomes zero is closely approximated by Equation 1. If minor axis bending and warping restraints are present at the critical segment ends, the stiffness matrix must be modified by the addition of non-dimensionalised restraint stiffness to the appropriate terms and a higher buckling load can be expected. The adjacent segments in the substructure provide such restraint.

4.2 Restraint Stiffnesses

In an I-beam with major axis moment, minor axis bending and warping actions are coupled. Reactive minor axis moments and bimoments at fixities have been discussed in relation to Fig. 6 and the formation of a segment stiffness matrix. Coupling should be accounted for when assessing the end stiffnesses of a restraining segment. However, in order to simplify the behaviour of the substructure it is assumed that these actions are uncoupled at both ends of a restraining setment. For example, the minor axis bending stiffness at a restraining segment end is found by applying an end moment while allowing free warping at both ends. The appropriate boundary condition for bending is imposed at the far end. Stiffness additions are made therefore only to the diagonal terms of the critical segment stiffness matrix.

Variations in uncoupled minor axis bending stiffnesses at end A of a restraining segment are shown in Fig. 9. The stiffnesses depend on the far end boundary conditions and on the values of M/M_E, β and K. The reduction in stiffness with increasing major axis moment is more pronounced at end A which has the larger major axis end moment, M.

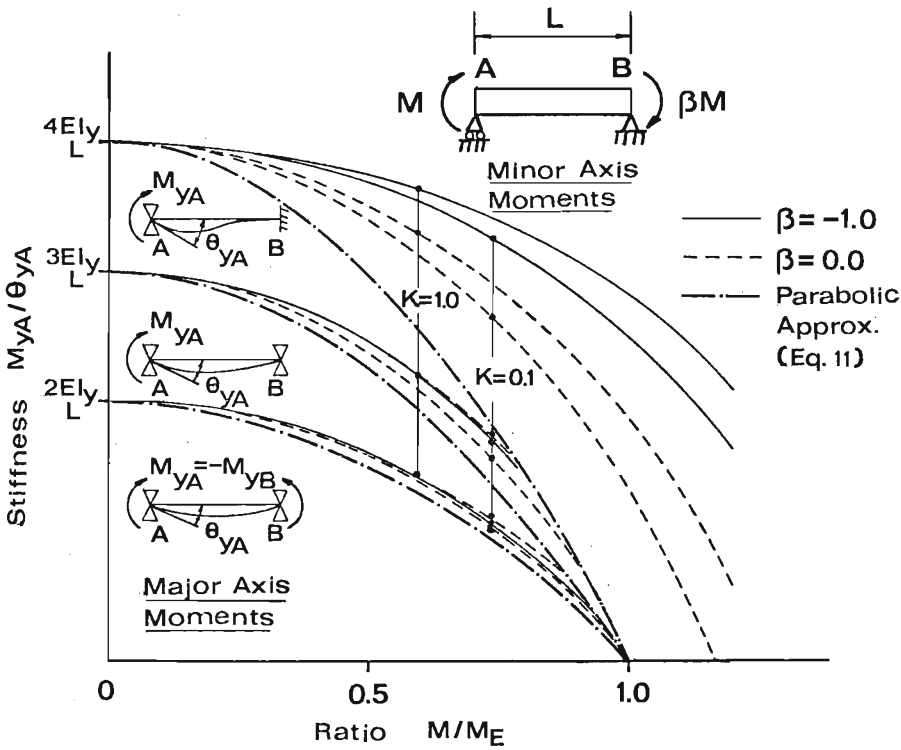

FIGURE 9 : Variations in minor axis bending stiffness

It has been shown (16) that most curves in the range $M/M_E < 1.0$ can be conservatively and adequately represented by parabolic approximations,

$$\text{Uncoupled bending stiffness} = n \left(\frac{EI_y}{L}\right)_R \left[1 - \left(\frac{M}{M_E}\right)^2\right]_R \qquad (11)$$

where the subscript, R, refers to a restraining segment and n = 2, 3 or 4. If the far end is simply supported, n = 3 and if fixed against minor axis rotation, n = 4. When the segment continues on to another, n = 2 in accordance with the assumed boundary condition of an equal restraint demand at the far end

producing single curvature bending. In some beams, restraining segments with high values of β buckle with reverse curvature and the assumed value of n = 2 may be over-conservative. As this depends on both β and the acutal restraint demand, no precise rule on the use of other n values (eg. n = 6) has been formulated.

Variations in uncoupled warping stiffnesses at end A of the segment are shown in Fig. 10. Again the stiffnesses depend on the far end boundary condtions, M/M_E, β and K, and differ from one end to the other (16). The parabolic approximations in Equation 11 are conservative (16) and have the same form as the bending stiffness approximations.

$$\text{Uncoupled warping stiffness} = n\left(\frac{EI_\omega}{L}\right)_R \left[1 - \left(\frac{M}{M_E}\right)^2\right]_R \qquad (12)$$

where the values of n are assumed to be 2, 3 or 4 depending on the far end boundary condition. The true value of n varies with the beam parameter, K, (see Fig. 10) and approaches 2, 3 or 4 only when K is large. In slender beams where warping interaction is not significant the assumed values of n, although incorrect, are of minor importance. The significance of warping increases with the value of K as does the accuracy of the assumed values.

4.3 Substructure Stiffness Matrix

The critical segment stiffness matrix in Equation 9 may be modified by the addition of restraining segment end stiffnesses to the diagonal terms to form a substructure stiffness matrix,

$$\begin{bmatrix} S_{11} + \frac{2}{G_A} & S_{12} & S_{13} & S_{14} \\ S_{21} & S_{22} + \frac{2}{G_A} & S_{23} & S_{24} \\ S_{31} & S_{32} & S_{33} + \frac{2}{G_B} & S_{34} \\ S_{41} & S_{42} & S_{43} & S_{44} + \frac{2}{G_B} \end{bmatrix} \qquad (13)$$

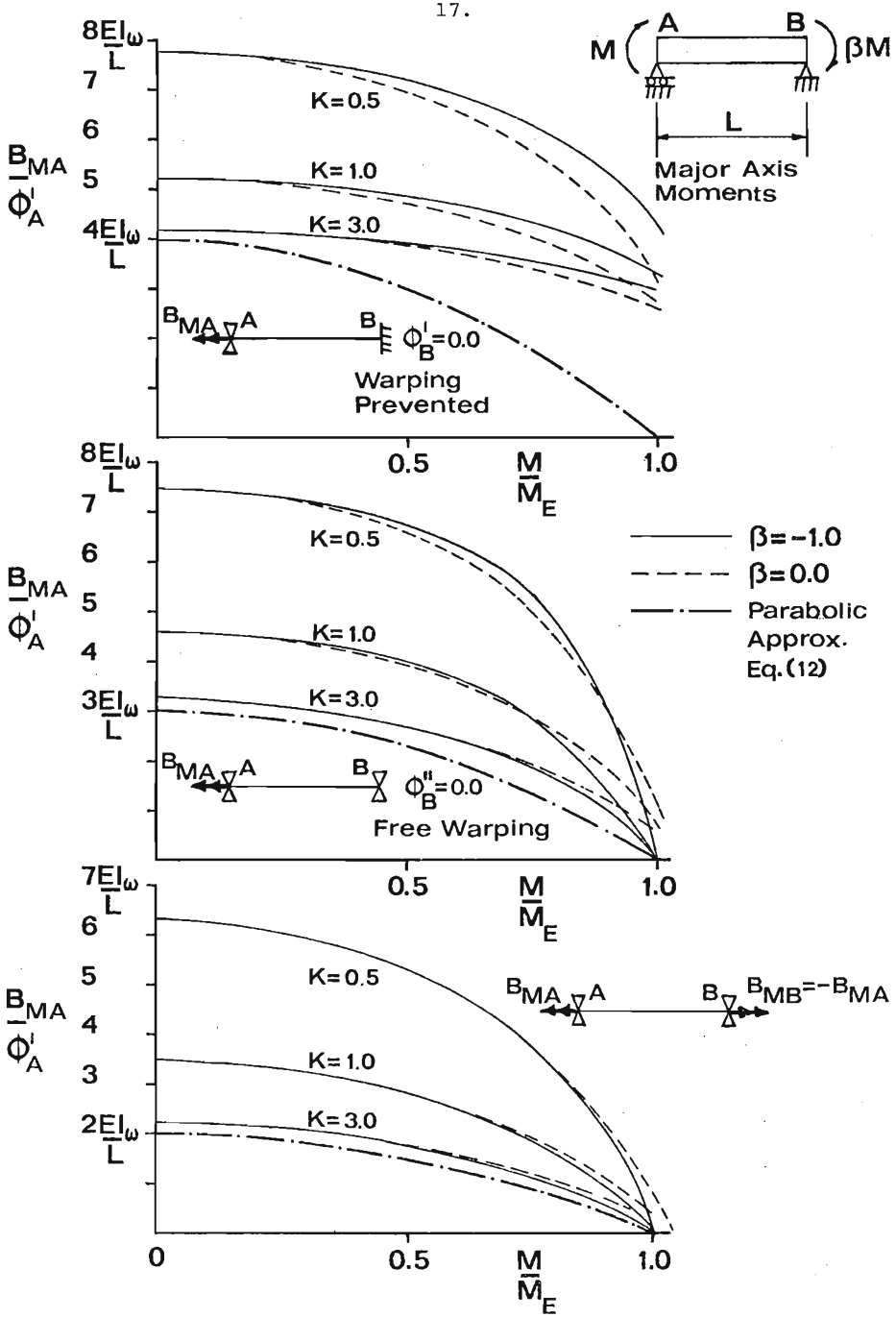

FIGURE 10 : Variations in warping stiffness

In Equation 13, the restraint additions are expressed as $2/G_A$ and $2/G_B$. Stiffnesses of the types in Equations 11 and 12 cannot be added directly to the dimensionless critical segment matrix but must be altered to suit the forces and displacements in Equation 10. The restraint parameters G_A and G_B are

$$G_{A,B} = \frac{2\left(\frac{EI_y}{L}\right)_C}{n\left(\frac{EI_y}{L}\right)_R\left[1 - \left(\frac{M}{M_E}\right)^2\right]_R} \qquad (14)$$

where the subscript, C, refers to the critical seqment. It is assumed that, for the far end of a restraining segment, the boundary conditions for warping and minor axis bending are the same. Furthermore, it is assumed that the ratios of minor axis bending rigidities and warping rigidities are identical, that is

$$\frac{\left(EI_y\right)_C}{\left(EI_y\right)_R} = \frac{\left(EI_\omega\right)_C}{\left(EI_\omega\right)_R} \qquad (15)$$

Therefore a single restraint parameter represents both the warping and the bending restraints at a critical segment end.

4.4 Effective Length Factors

Using the foregoing process the substructure is reduced to a critical segment with load dependent end restraints. For given values of beam parameter, K, and moment gradient, β, in the critical segment, and for a given pair of restraint parameters G_A and G_B, the diminsionless elastic buckling moment, γ_F, may be obtained by finding the critical segment moment ratio, $(M/M_E)_C$, at which the substructure stiffness matrix determinant first becomes zero.

$$\gamma_F = \frac{M_F L}{\sqrt{EI_y GJ}} = \text{fn}\left(K, \beta, G_A, G_B\right) \tag{16}$$

where $(M/M_E)_C$ equals $(M_F/M_E)_C$ at buckling.

By introducing an effective length factor, k, for the critical segment the dimensionless moment may be written following Equation 1,

$$\gamma_F = \frac{\pi}{k}\sqrt{1 + \left(\frac{K}{k}\right)^2} \tag{17}$$

that is

$$k = \frac{\pi}{\sqrt{2}\gamma_F}\sqrt{1 + \sqrt{1 + \left(\frac{2\gamma_F K}{\pi}\right)^2}} = \text{fn}\left(K, \beta, G_A, G_B\right) \tag{18}$$

Rather than to search for γ_F, an alternative is to nominate k (hence γ_F), K, β and either G_A or G_B and to calculate the other restraint parameter necessary for a zero determinant. The determinantal equation is a simple quadratic in the unknown restraint parameter.

A number of effective length factor charts have been prepared for β = -1.0, -0.75, -0.5, -0.25, 0.0, 0.25, 0.5, 0.75, 0.9 and 1.0 and for K = 0.1, 0.3, 0.5, 1.0 and 3.0, and are given in Figs. 11 to 20. It should be emphasised again that end A of the critical segment AB has the larger major axis end moment and that G_A refers to this end.

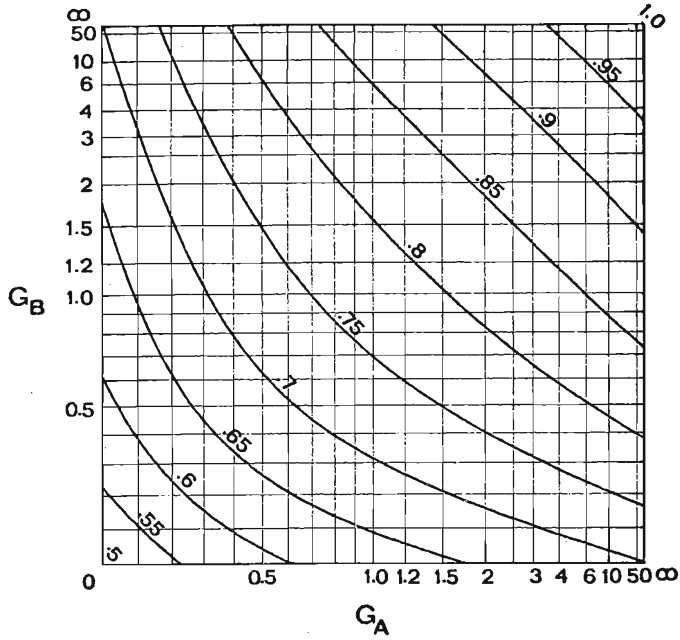

FIGURE 11

$\beta = -1.0$

All K Values

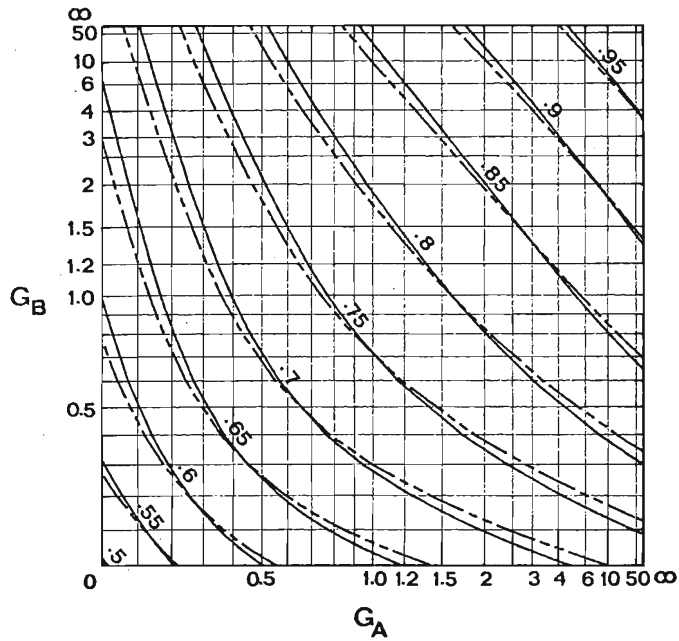

FIGURE 12

$\beta = -.75$

——— K=0.1

— — — =3.0

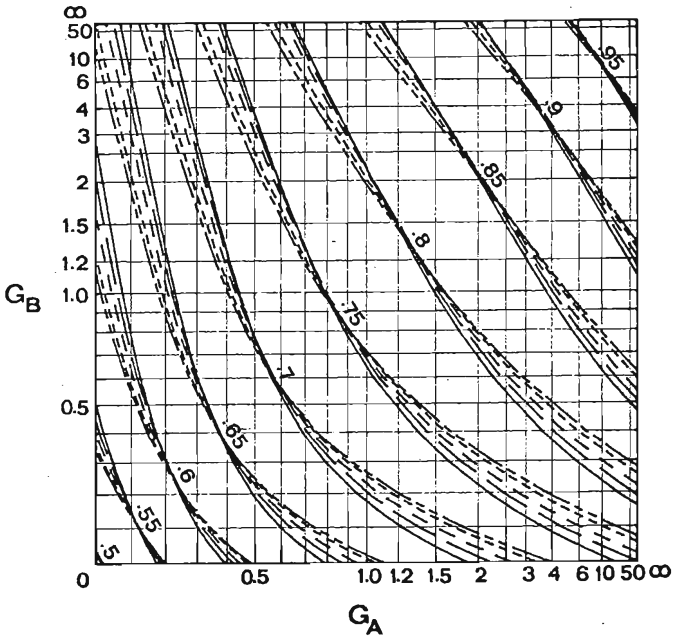

FIGURE 13

$\beta = -.5$

K = 0.1
= 0.3
= 0.5
= 1.0
= 3.0

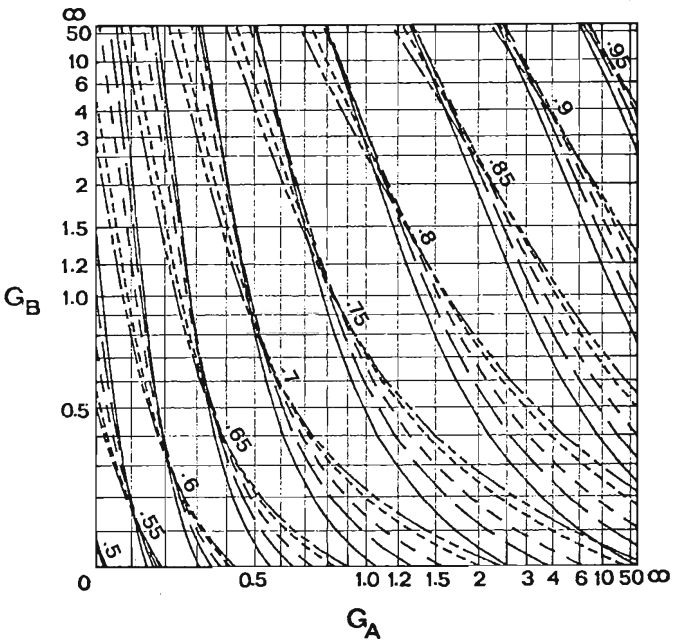

FIGURE 14

$\beta = -.25$

K = 0.1
= 0.3
= 0.5
= 1.0
= 3.0

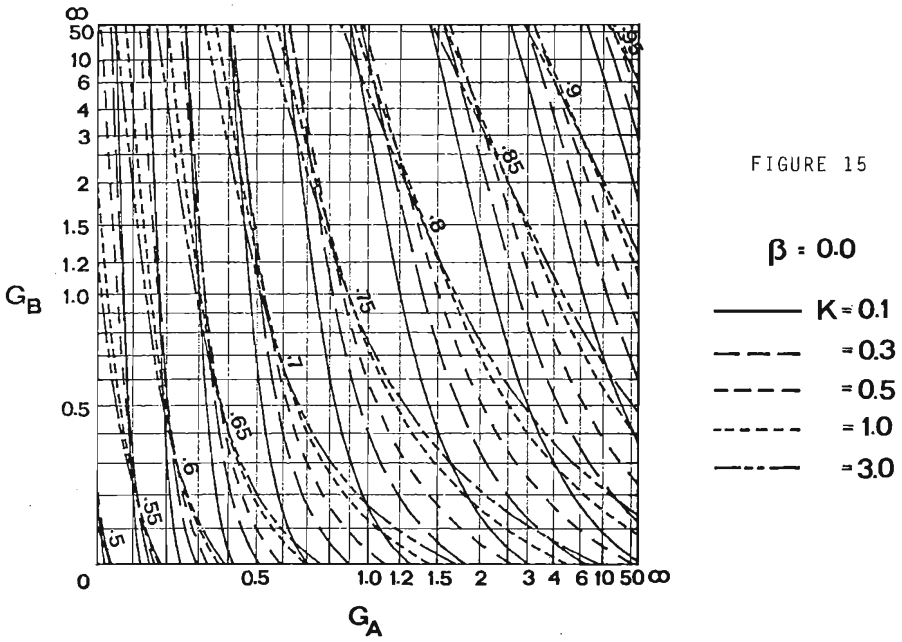

FIGURE 15

The following general points may be made:

(1) The factors, k, are not generally independent of the beam parameter, K, and the moment gradient, β, as assumed by Nethercot and Trahair (1-3). This assumption will be discussed more fully in a later section.

(2) When β = -1.0, the effective length curves are independent of the beam parameter, K. The effective length chart in Fig. 11 is, in fact, identical to the column effective length chart for the sway prevented case. For all other β values the effective length factor, k, associated with a particular set of end restraint parameters, G_A and G_B, is dependent on the beam parameter, K. This becomes more pronounced as the moment gradient, β, increases.

(3) When β = -1.0 or +1.0 the restraint parameters, G_A and G_B, have equal effectiveness. The effective length curves are symmetrical about the diagonal from lower left

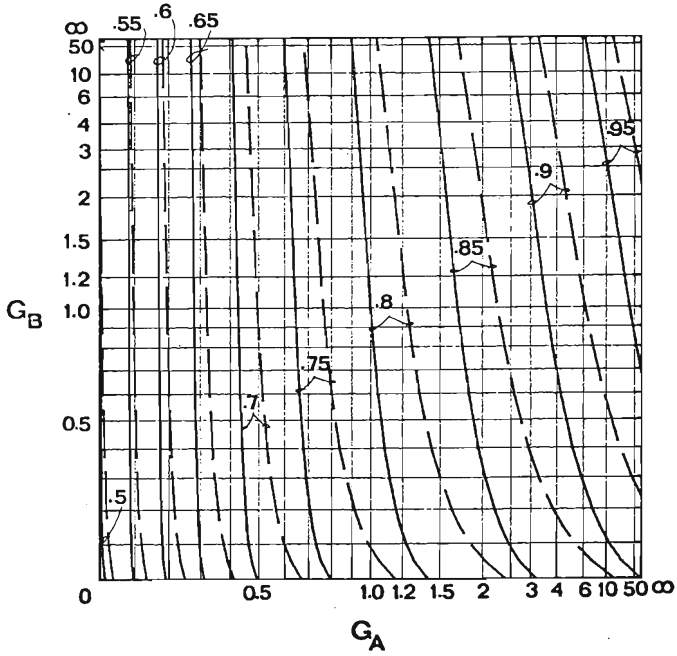

FIGURE 16(a)

$\beta = +.25$

——— K = 0.1

—·—·— = 0.3

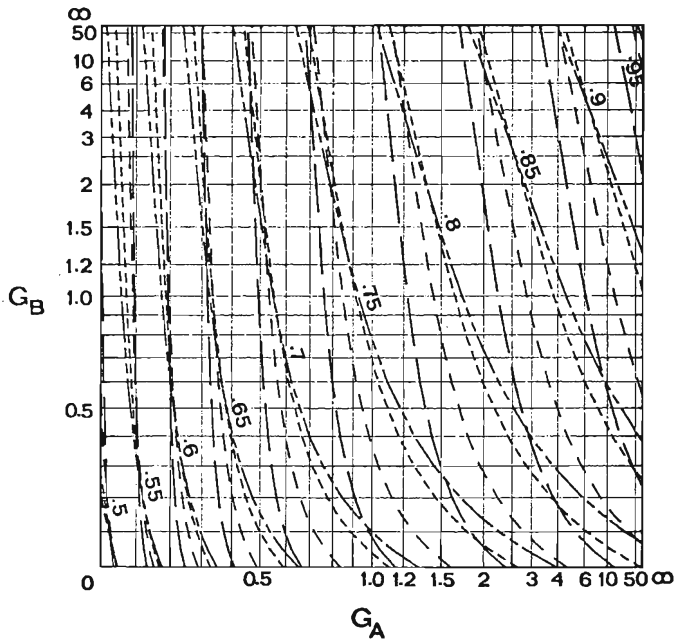

FIGURE 16(b)

$\beta = +.25$

— — — K = 0.3

— — — — = 0.5

------- = 1.0

—·—·— = 3.0

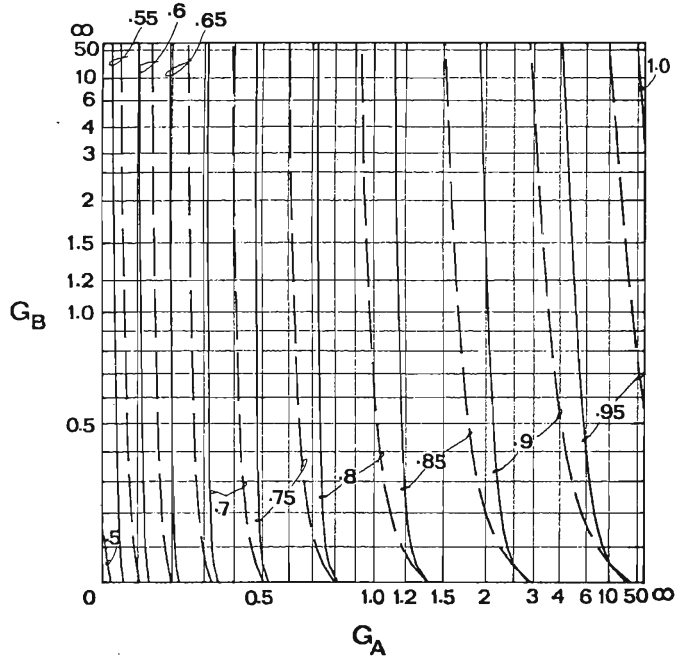

FIGURE 17(a)

$\beta = +.5$

——— K = 0.1

— — — = 0.3

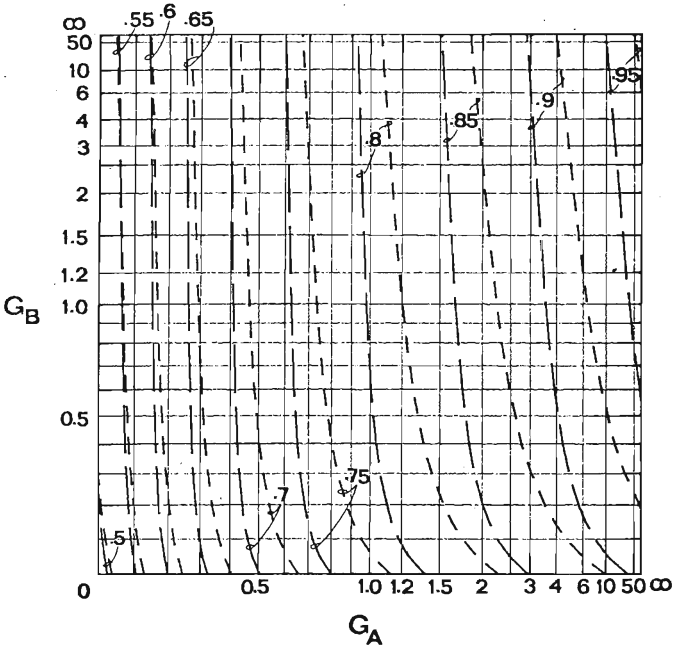

FIGURE 71(b)

$\beta = +.5$

— — — K = 0.3

— — — = 0.5

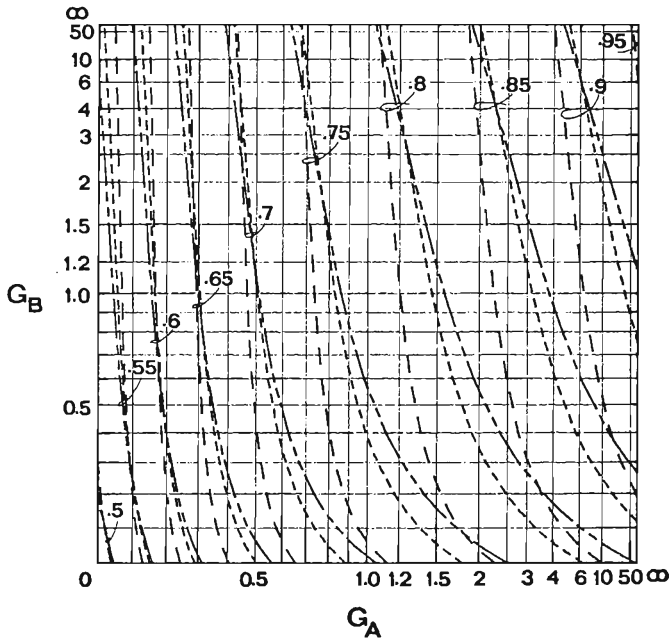

FIGURE 17(c)

$\beta = +.5$

———— K = 0.5

------ = 1.0

—·—·— = 3.0

(G_A = G_B = 0.0) to upper right (G_A = G_B = ∞). In the range between these two gradients a restraint at end A of the critical segment has the greater significance. The reduction in influence of a restraint at end B is associated mainly with changes in the minor axis rotation mode shape and, to a lesser extent, with changes in the warping mode shape. Some mode shapes have been obtained by Finite Element analysis (9) and are shown, in normalised form, in Fig. 21 (see page 32). When β = -1.0 the minor axis rotation mode shape is anti-symmentrical (Fig. 21(b)). The lateral displacement shape is symmetrical with single curvature (Fig. 21(a)). When β = +1.0 the rotation mode shape is symmetrical with two internal nodes, corresponding to an anti-symmetrical lateral displacement mode shape with double curvature. Between the limits of β, the mode shapes are changing from the one set to the other and, in comparison with conditions at end A, considerably less and even zero rotation might occur at end B. Consequently, a bending restraint at end B may have little influence.

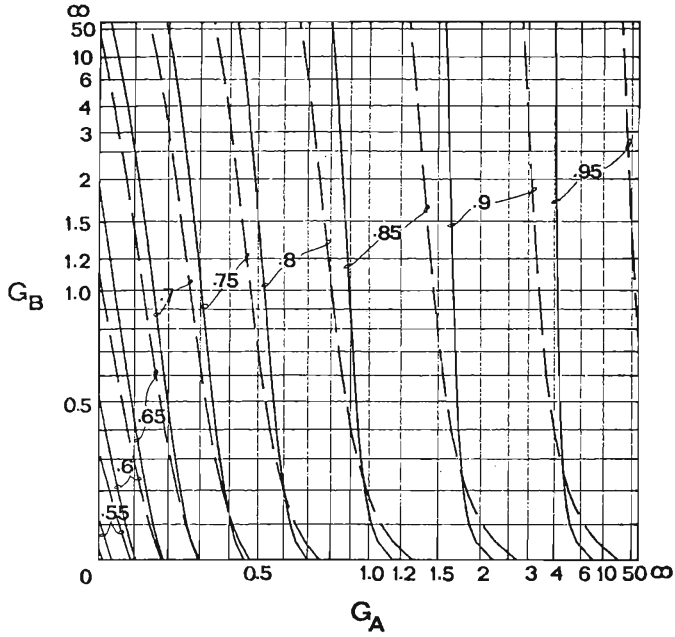

FIGURE 18(a)

$\beta = +.75$

——— K = 0.1

— — — = 0.3

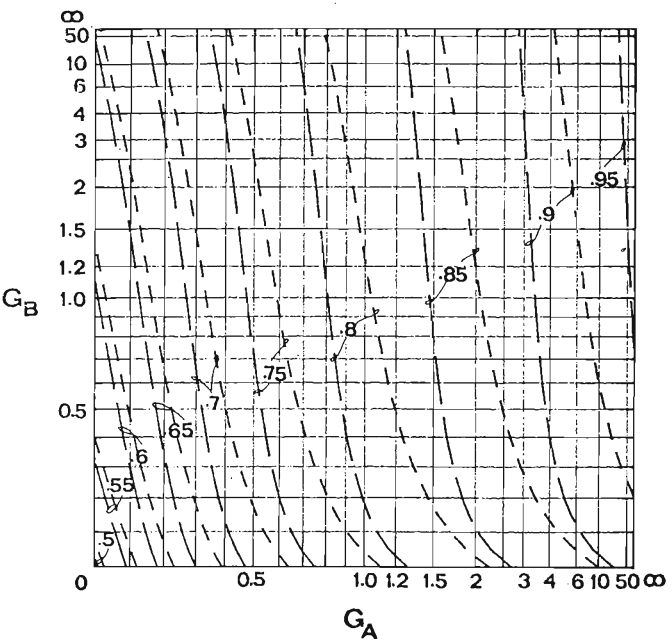

FIGURE 18(b)

$\beta = +.75$

— — — K = 0.3

— — — — = 0.5

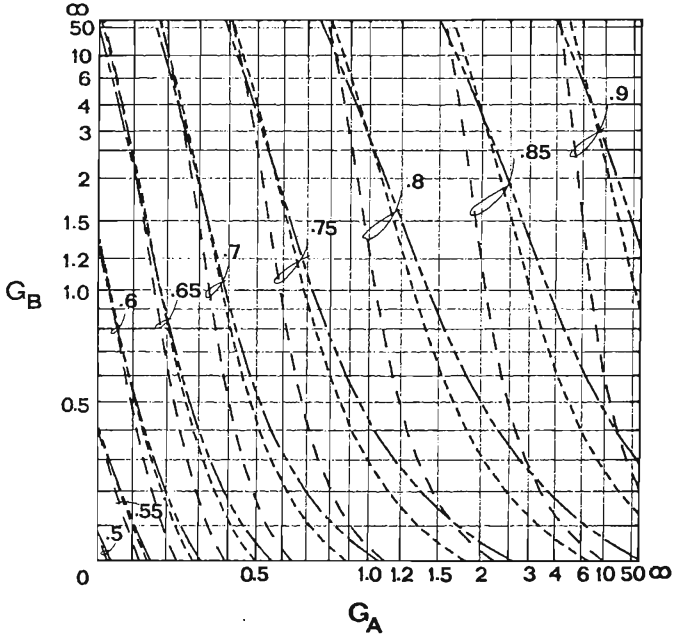

FIGURE 18(c)

β = +.75

---- K = 0.5

------- = 1.0

—··— = 3.0

In Fig. 21(c), the angle of twist, ϕ, retains a single curvature mode shape which is symmetrical at the limits $\beta = -1.0$ and $\beta = 1.0$. For intermediate values of β the shape is slightly more pronounced near end A. The warping displacements at a cross-section are proportional to the first derivative of the angle of twist, ϕ', (17) and mode shapes are given in Fig. 21(d). The effect of restraining the warping displacements at a segment end depends, in the first instance, on the beam parameter, K (19). Variations in the relative warping displacements of ends A and B with moment gradient, β, (see Fig. 21(d)) indicate that a warping restraint is more effective when acting at end A. Nevertheless a restraint end B retains influence throughout the full range of β, as ϕ'_B does not undergo such severe alteration as does the minor axis rotation at this end.

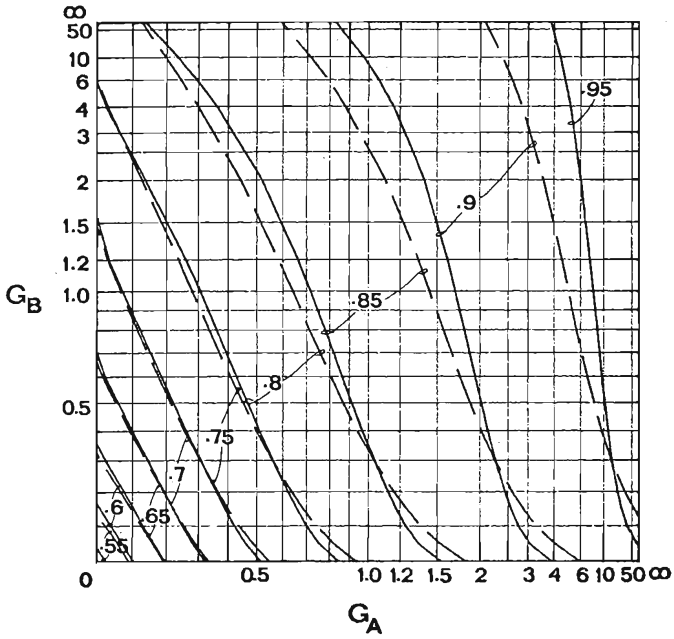

FIGURE 19(a)

$\beta = +.9$

——— K = 0.1

— — — = 0.3

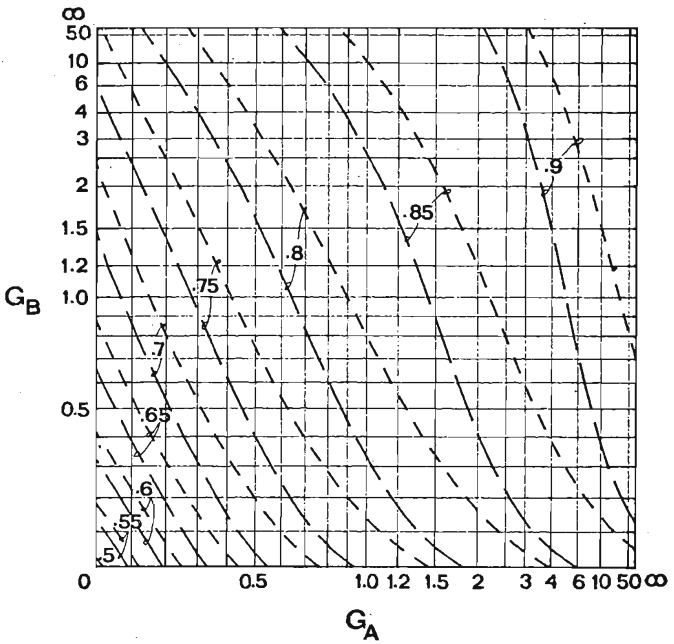

FIGURE 19(b)

$\beta = +.9$

— — — K = 0.3

— — — = 0.5

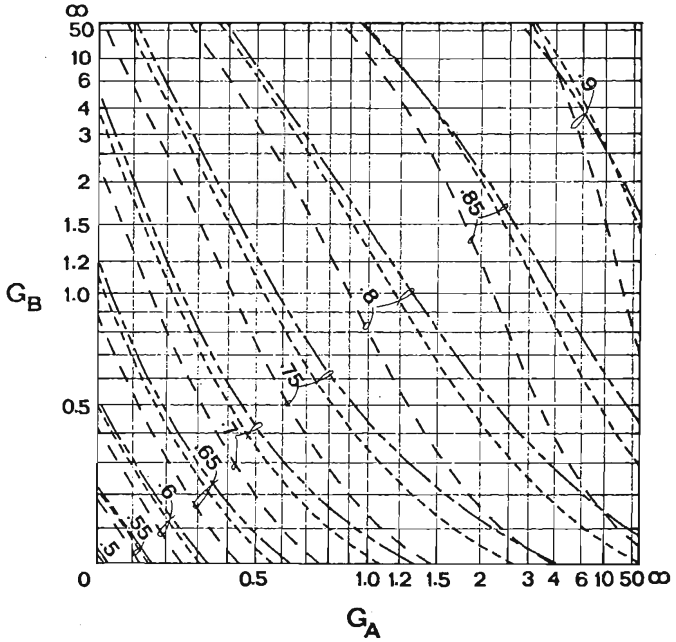

FIGURE 19(c)

(4) The moment modification factor, m, (Equation 3) is approximate and its true value depends not only on the moment gradient β, but also on the beam parameter, K (12). This is particularly so for higher moment gradients ($\beta > 0.0$). The inaccuracies in Equation 3 have been compensated for in the effective length charts. The factor, m, is usually conservative and for many pairs of β and K, the effective length curve for $k = 1.0$ and even for $k = 0.95$ lies outside the upper right hand corner of the charts. These curves have not been plotted. In some instances the factor, m, is unconservative and a curve for $k = 1.0$ appears on the charts.

(5) The effective length factor, k, has a lower bound of $k \approx 0.5$ but some variation is evident. This is generally attributable to the approximate nature of the moment modification factor m. The lower bound is established by examining the terms of the critical segment stiffness matrix as k decreases. It is possible to determine

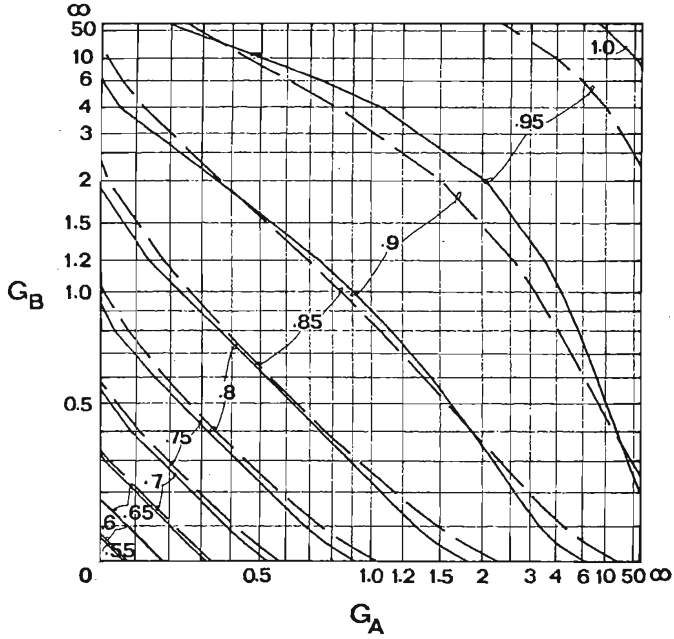

FIGURE 20(a)

$\beta = +1.0$

——— K = 0.1

– – – = 0.3

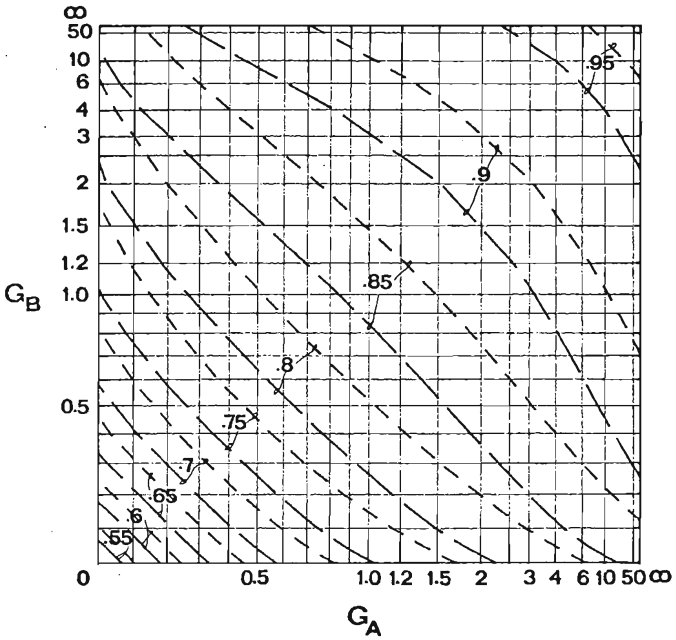

FIGURE 20(b)

$\beta = +1.0$

– – – K = 0.3

– – – – = 0.5

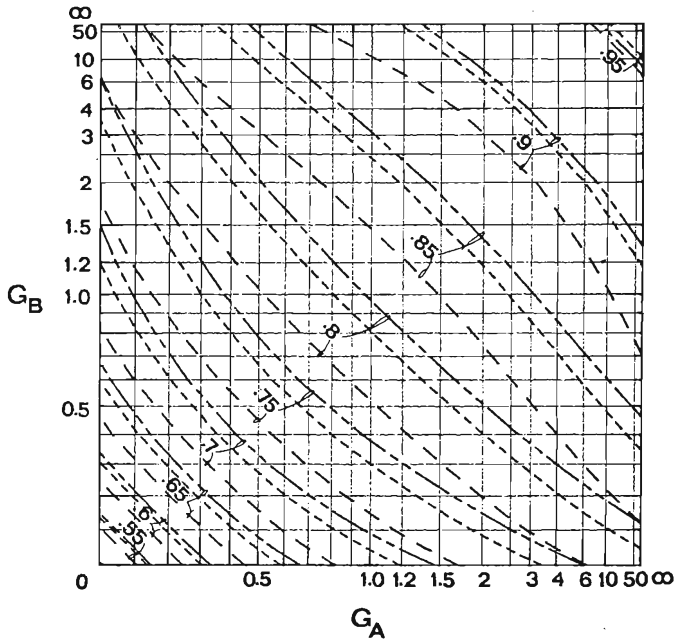

FIGURE 20(c)

β = +1.0

K = 0.5

= 1.0

= 3.0

whether or not adequate parameters G_A and G_B, can be provided with the critical segment still buckling in its lowest mode.

(6) The listed values of β and K have been chosen to cover the full moment gradient range for slender critical segments (K = 0.1) to very stocky ones (K = 3.0). Linear interpolation may be used for segments having other β and K values. Alternatively, the nearest set of conservative curves may be chosen to represent the behaviour of the segment and this set can be found by inspection of the charts. This second approach is recommended when β approaches +1.0 as marked changes occur in the effective length curves for small changes in β. Charts for β = +0.9 have been included to assist in the determination of k for high moment gradient segments.

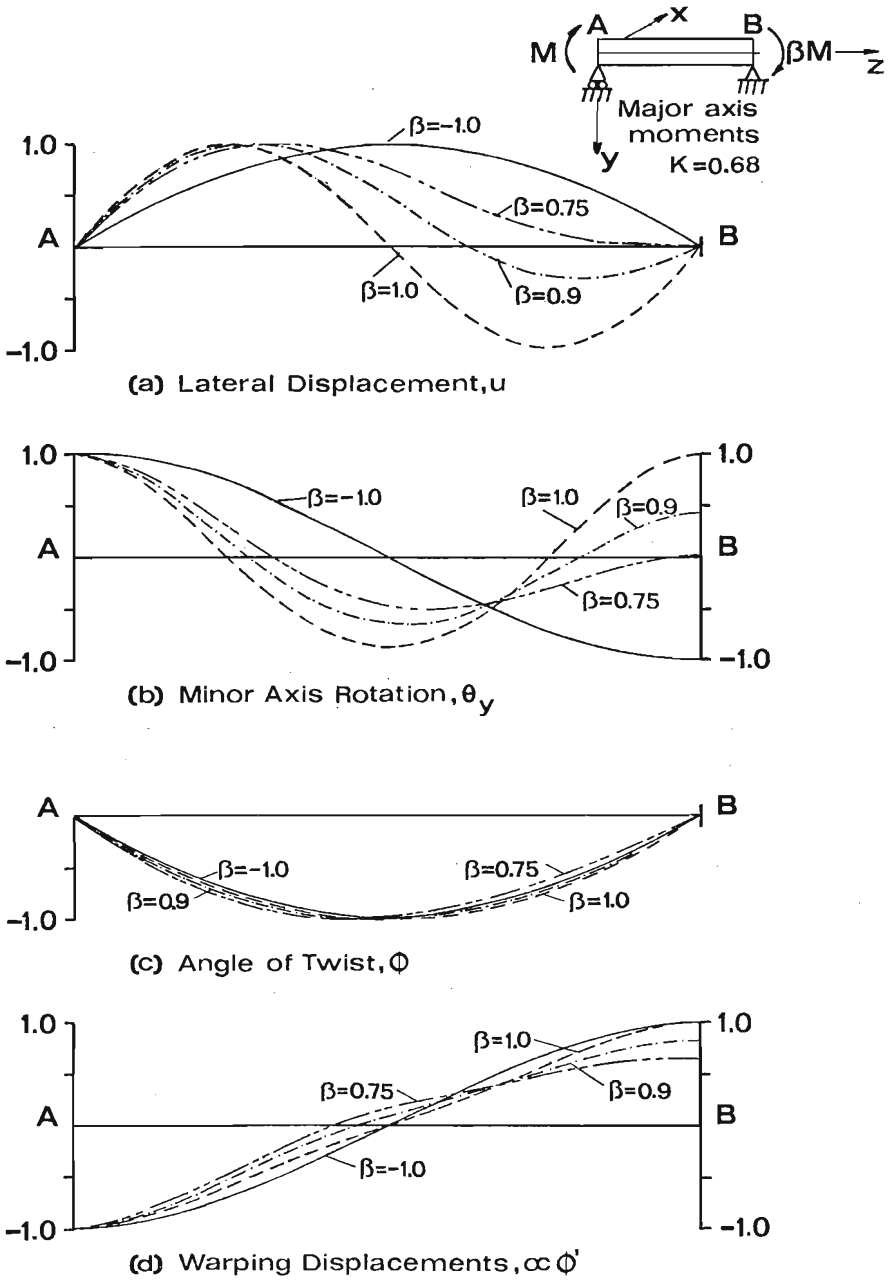

FIGURE 21 : Normalised mode shapes

5. ANALYSIS PROCEDURE

5.1 Summary of Steps

The procedure for determining the elastic buckling load of a laterally continuous beam can be summarised as follows:

(1) Determine the major axis bending moment distribution.

(2) Determine K and β for each segment.

(3) For each segment calculate M_E from Equation 1 and the corresponding beam load factor, λ, to produce M_E. The segment with the lowest load factor, λ_C, is the critical segment. The two (at most) adjacent segments have higher load factors, λ_R.

(4) Assume a trial value of λ_F, the load factor at substructure buckling, and calculate G_A and G_B from Equation 13. Note that

$$\frac{\lambda_F}{\lambda_R} = \left[\frac{M}{M_E}\right]_R \tag{19}$$

and this substitution may be made in Equation 13. The trial value of λ_F should lie between λ_C and λ_R (min).

(5) Find the critical segment effective length factor, k, using the appropriate chart from Figs. 11 to 20, extrapolating linearly if necessary.

(6) Calculate the revised critical segment buckling moment, M_F, from Equations 16 and 17, and obtain a new load factor, λ_F (new).

Note that

$$\frac{\lambda_F(\text{new})}{\lambda_C} = \left[\frac{M_F}{M_E}\right]_C \tag{20}$$

(7) Compare the new load factor, λ_F(new), with the assumed factor, λ_F (Step 4), and repeat Steps 4 to 6 if necessary until good agreement is obtained.

The process of cycling ensures consistency between assumed values at Step 4 and calculated values at Step 6. Usually only two or three cycles are required if a reasonable initial guess for λ_F is made at Step 4. Converging upper and lower bounds are found by choosing an initial value of λ_F equal to λ_C and subsequent values of λ_F equal to those calculated at Step 6.

It is conceivable that at Step 3, more than one segment may have low load factors of similar value. The weakest segment may have stronger adjacent segments than the others in this group so, if in doubt, the designer should proceed with multiple analyses assuming different critical segments and subassemblages for each case.

5.2 Worked Examples

5.2.1 Example 1

The analysis procedure is applied to the beam in Fig.22.

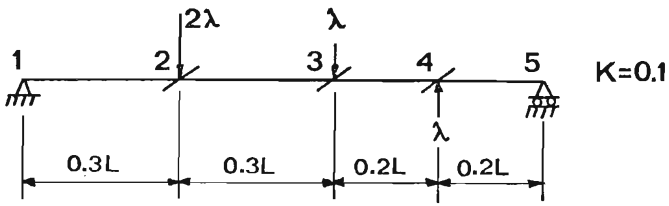

FIGURE 22 : Laterally continuous beam

Step 1. Calculate bending moments

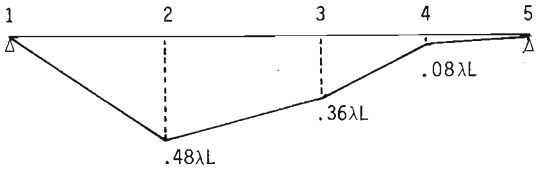

Step 2. Find β and K for each segment

	1	2	3	4	5
β =	0.0	-.75	-.222	0.0	
K =	.33	.33	.5	.5	

Step 3. Calculate M_E and load factors, λ, to produce buckling in simply supported segments.

	1	2	3	4	5	
M_E =	19.3	12.46	26.9	30.7		All multiplied by $\sqrt{EI_y GJ}/L$
λ =	40.21	25.96	70.72	384.12		All multiplied by $\sqrt{EI_y GJ}/L^2$

Segment 2-3 is the critical segment. The subassemblage consists of segments 1-2, 2-3 and 3-4.

Step 4. Assume a value of λ_F and calculate G_A and G_B. End 2 of the critical segment is taken as end A. Usually a close guess can be made for λ_F from the information gathered at Step 3, but for purposes of this example, an initial value of 25.96 $\sqrt{EI_y GL}/L^2$ will be used.

$$\therefore G_A = \frac{2}{3} \times \frac{.3L}{.3L} \times \frac{1}{\left[1-\left(\frac{25.96}{40.21}\right)^2\right]} = 1.14$$

$$\text{and } G_B = \frac{2}{2} \times \frac{.2L}{.3L} \times \frac{1}{\left[1-\left(\frac{25.96}{70.72}\right)^2\right]} = .77$$

Step 5. Find the critical segment effective length factor from the curves for $\beta = -.75$ and $K = .33 \approx .3$ in Fig. 12.

Effective length factor, k, = 0.76

Step 6. Calculate the revised critical segment buckling moment, M_F, and corresponding load factor, λ_F.

$$M_F = \frac{1.13\pi}{.3L \times .76} \sqrt{EI_y GJ} \sqrt{1+\left(\frac{.33}{.76}\right)^2}$$

$$= 17 \sqrt{EI_y GJ}/L$$

and $$\lambda_F = 35.36 \sqrt{EI_y GJ}/L^2$$

The following tabulation shows the convergence of λ_F. Although four cycles have been used in the tabulation, fewer would be adequate for this particular analysis.

Cycle	λ_F	G_A	G_B	k	λ_F(new)
1	25.96	1.14	.77	.76	35.36
2	35.36	2.94	.889	.82	32.40
3	32.40	1.90	.843	.79	33.80
4	33.80	2.27	.864	.81	33.0

i.e. $\lambda_F \approx 33.4 \sqrt{EI_y GJ}/L^2$

A finite integral analysis (10) gives

$$\lambda_F = 34.91 \sqrt{EI_y GJ}/L^2$$

The approximate value is conservative by 4.5%. This is due in part to the boundary condition imposed at brace 4 where it has been assumed that segment 4-5 places a restraint demand equal to that of the critical segment at brace 3. An inspection of the values of λ at Step 3 shows that segment 4-5 restrains

rather than destabilises segment 3-4, and that segment 3-4 is consequently stiffer than assumed.

The analysis can be refined in the following way to take advantage of this. After Step 3 and before Step 4, the load factor, λ_F, to produce buckling in the simply supported substructure 3-4-5 is calculated. The process follows that already outlined. The solution, λ_F, replaces λ_R for segment 3-4 in the analysis of the substructure 1-2-3-4. The revised value of λ_R is used in calculations of the restraint parameter G_B at Step 4. The value of n = 2 for segment 3-4 should also be revised as, since restraint is offered by segment 4-5, n must lie in the range $3 \leqslant n \leqslant 4$.

In many analyses the extra calculations have only marginal benefit, particularly when the restraining segment at end B of the critical segment is involved. In Example 1, the prediction is increased to $\lambda_F \approx 34\sqrt{EI_yGJ}/L^2$ and the error is reduced to a little under 3%. However, when the restraining segment at end A has a well restrained or fixed far end, it is advisable to use this refinement. This is demonstrated in the following example.

5.2.2 Example 2

A cantilever with a tip load and an additional internal brace is shown in Fig. 23.

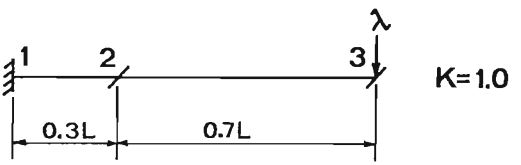

FIGURE 23 : Braced cantilever with tip load

Step 1. Calculate bending moments

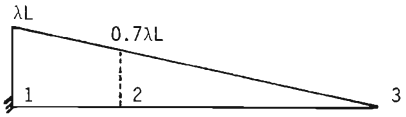

Step 2. Find β and K for each segment

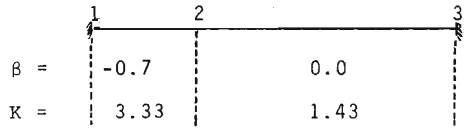

Step 3. Calculate M_E and load factors, λ, to produce buckling in simply supported segments.

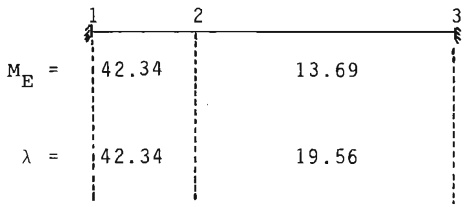

Step 3. (revised) Calculate M_E and load factor, λ, to produce buckling in substructure 1-2.

$G_A = 0.0$ (end 1 is fully fixed)

$G_B = \infty$ (end 2 is simply supported)

From the effective length curves for $\beta = -.75$ and $K = 3.0$ in Fig. 12.

Effective length factor, k, = 0.68

Hence,

	1	2	3	
M_E =	89.4	13.69		All multiplied by $\sqrt{EI_y GJ}/L$
λ	89.4	19.56		All multiplied by $\sqrt{EI_y GJ}/L^2$

Step 4. Estimate $\lambda_F \approx 38$

$$\therefore G_A = \frac{2}{4} \times \frac{.3L}{.7L} \frac{1}{\left(1-\left(\frac{38}{89.4}\right)^2\right)} = .261$$

$$G_B = \infty$$

Step 5. Find the critical segment effective length factor from Fig. 15 ($\beta = 0.0$).

$$k = .675$$

Step 6. Calculate the revised critical segment buckling moment and corresponding load factor.

$$M_F = 27.24 \sqrt{EI_y GJ}/L$$

and

$$\lambda_F = 38.9 \sqrt{EI_y GJ}/L^2 \quad \text{cf } 38 \sqrt{EI_y GJ}/L^2$$

A value of 38.45 is a reasonable compromise. The standard procedure leads to a value of 32.5 whereas a Finite Integral analysis (10) gives

$$\lambda_F = 37.6 \sqrt{EI_y GJ}/L^2$$

The refined solution overestimates the buckling load by 2% and the standard solution underestimates it by 9%.

6. COMPARISON WITH ALTERNATIVE METHODS

Salvadori (13) has proposed a lower bound approach which neglects interaction between segments. The analysis stops at Step 3 with the calculation of λ_C which is taken to be the beam load factor at failure. The disadvantages of this approach have been noted by Nethercot and Trahair (1-3), and illustrated with the example in Figs. 3, 22 and 23.

The approximate method in this paper is a refinement of that proposed by Nethercot and Trahair (1-3). There are many common points, notably in the choice of a substructure and in the approach to solution using effective length factors and restraint parameters. However there are several major differences. Most importantly, Nethercot and Trahair propose a single set of effective length curves for all critical segments. This set is identical to that in Fig. 11 which should apply only to critical segments under uniform major axis bending. As a result no proper account is taken of the relationship between the effectiveness of an end restraint and both the critical segment moment gradient and the end at which the restraint is applied. Similarly the influence of the beam parameter is ignored. However an examination of the sets of effective length curves for negative moment gradients shows that, in the diagonal region from lower left to upper right ($G_A \approx G_B$) little variation occurs. Hence the assumption of a single set is not unreasonable if the critical segment moment gradient is less than zero and if the parameters G_A and G_B have similar values.

Nethercot and Trahair suggest a linear rather than a parabolic deterioration of restraining segment end stiffness. The function has the form $(1 - \lambda_C/\lambda_R)$ rather than $(1 - (\lambda_F/\lambda_R)^2)$ as recommended in this paper. The value of λ_C is found at Step 3 of the analysis procedure and, as cycling is not suggested, no revision of restraint parameters is made. As λ_C is often considerably less than λ_F, its use may compensate for the conservative linear function.

If these differences are incorporated in the procedure of section 5, analysis can proceed according to the method in References 1-3. Cycling is an option which may be introduced by replacing λ_C with λ_F, the current load factor.

7. APPLICATION TO PROBLEMS

Many structures have been analysed using the proposed method. Buckling load predictions have been compared with Finite Integral (11) and Finite Element (9) results and agreement is good. A selection of analysis results is presented in Figs. 24 to 29 which also includes predictions from the alternative hand methods (1-3, 13).

In Fig. 24, the braced cantilever in Example 2 is examined further as the internal brace is moved along the cantilever. The refinement concerning the effect of the end fixity on the stiffness of segment 1-2 when acting as a restraining segment (see Example 2) has been incorporated into both the proposed method and that of Nethercot and Trahair (1-2). When segment 1-2 is critical, the effect of the fixity is included in both standard methods. The segment buckling loads for Salvadori's method (13) have been calculated from Equation 2 and no account has been taken of the restraint offered to segment 1-2 by the end fixity. Buckling load estimates for this segment would be required from other sources or from one of the alternative hand methods in order to do this.

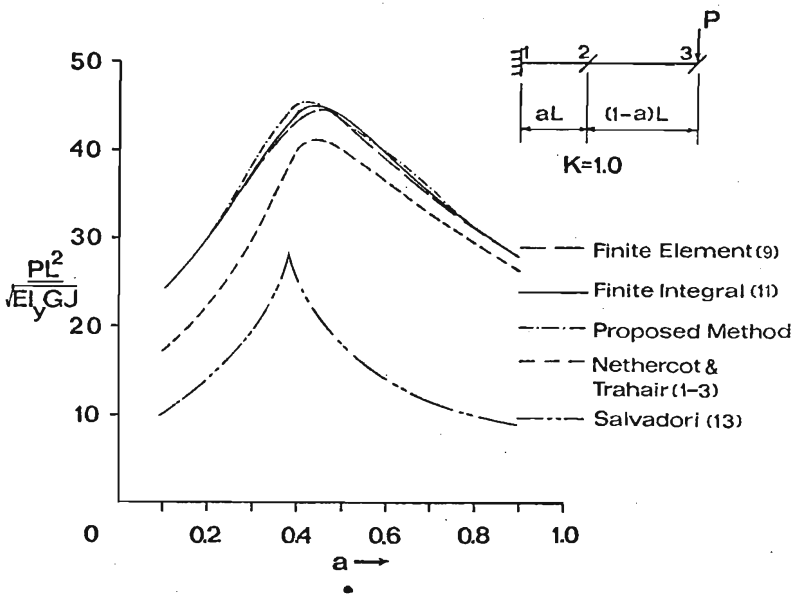

FIGURE 24 : Buckling loads for braced cantilever

Although all of the analyses predict an optimum internal brace location in the close range $0.38 \leqslant a \leqslant 0.46$, significant differences in the buckling load estimates are evident. The proposed method agrees well with the more precise solutions (9, 11), whereas the other hand methods (1-2, 13) underestimate the buckling loads by varying amounts.

The simply supported structures in Figs. 25 to 29 have been chosen from a series devised to test the accuracy of the proposed method when the solution point lies near an extreme of the relevant effective length chart. As the structures have only two segments, the analyses are free from approximations introduced by choosing a substructure. Where appropriate, pairs of structures have been selected such that a restraining segment is placed in turn at ends A and B of the critical segment. As this causes one of the restraint parameters, either G_B or G_A respectively, to be infinite, the solution point for the effective length factor, k, lies on a chart boundary.

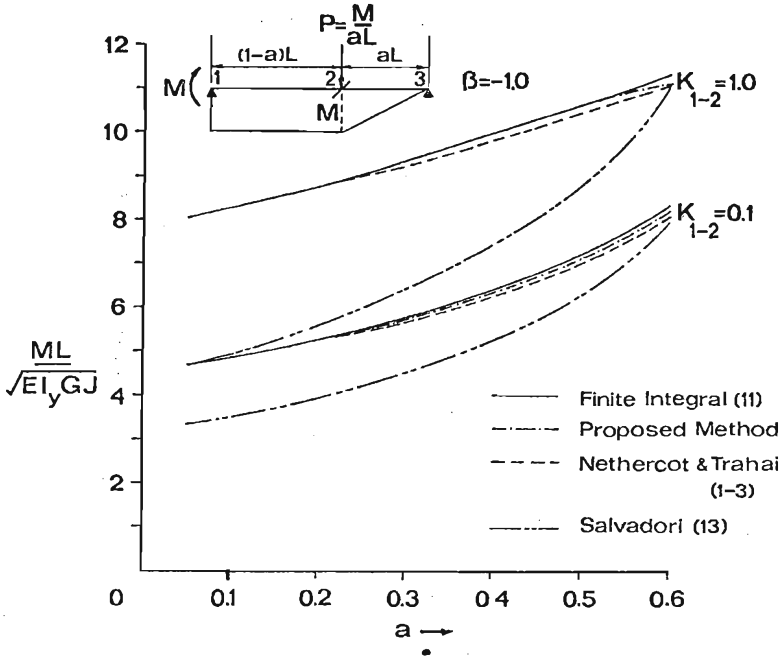

FIGURE 25 : Beam with end moment and point load

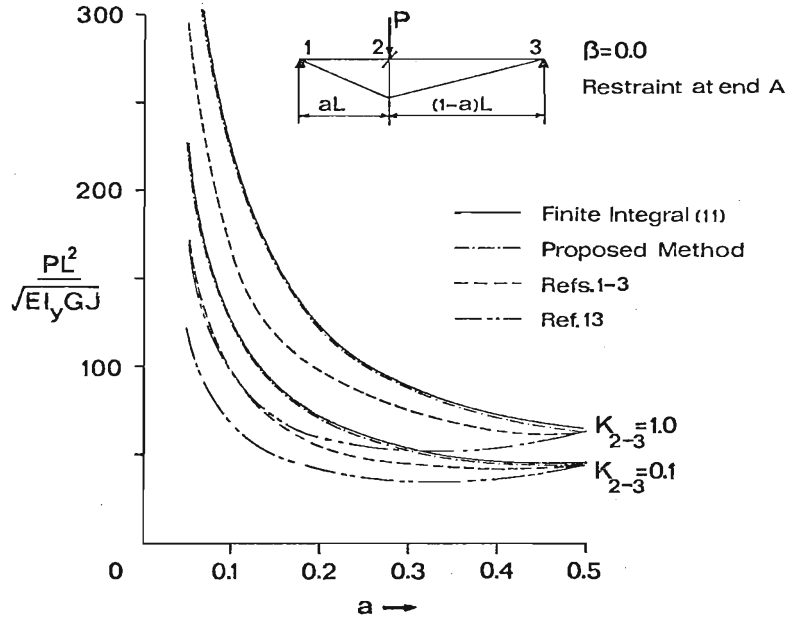

FIGURE 26(a) : Beam with point load

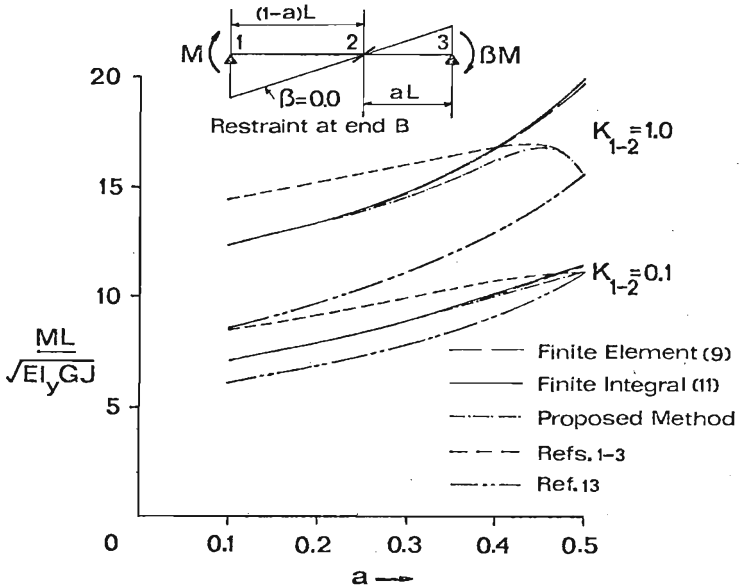

FIGURE 26(b) : Beam with end moments

Two critical segment beam parameters have been considered, K = 0.1 for a slender segment and K = 1.0 for a segment on which an end warping restraint can have considerable influence. Some general conclusions on the accuracy of the hand methods are made at the end of this section. One particular discrepancy occurs in Fig. 26(b) where all approximate methods underestimate the buckling moment as the internal brace approaches mid-span (a → 0.5). The methods predict no segment interaction when a = 0.5 and do this also for the structures in Figs. 27(a) and 27(c).

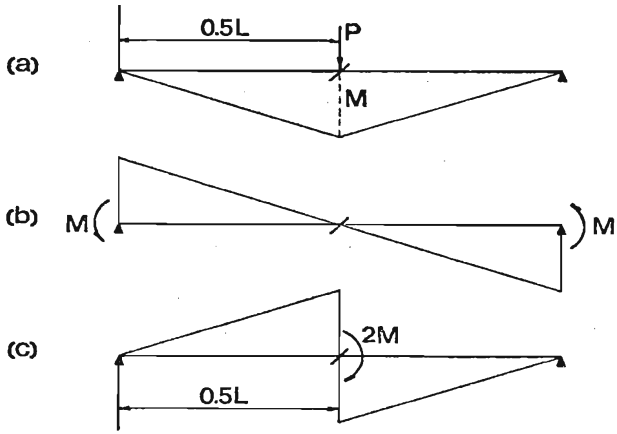

FIGURE 27 : Beams with segment moment gradients, β, = 0

It has been shown (16) that for the beam in Fig. 27(a), no interaction occurs and this is reaffirmed in Fig. 26(a) where all methods are in good agreement when a = 0.5. The behaviour of the structures in Figs. 27(b) and 27(c) differ markedly from this. The requirement of compatibility of nodal warping displacements at the internal brace results in the full suppression of warping at mid-span (16) and the segment moment levels at buckling are increased over that of the structure in Fig. 27(a). This effect is most pronounced for the beam in Fig. 27(c) where the internal warping restraint occurs at the maximum moment end.

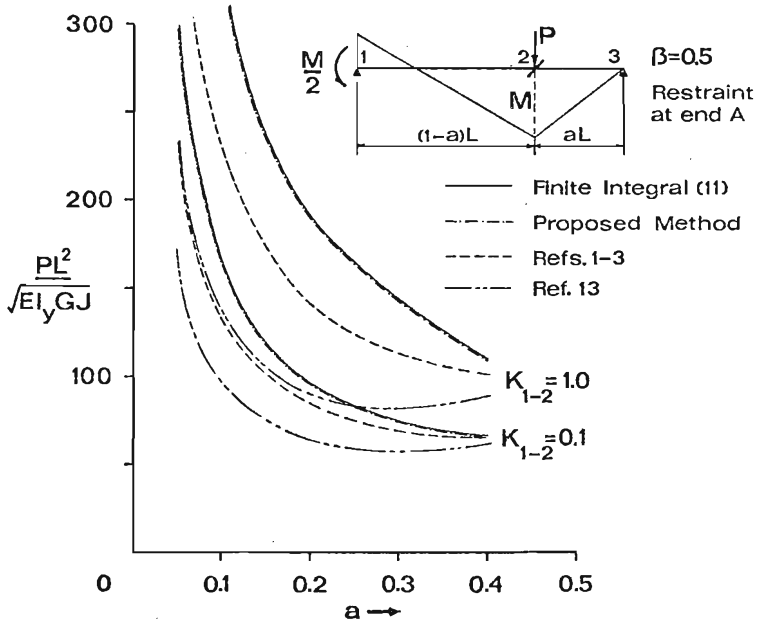

FIGURE 28(a) : Beam with point load and end moment

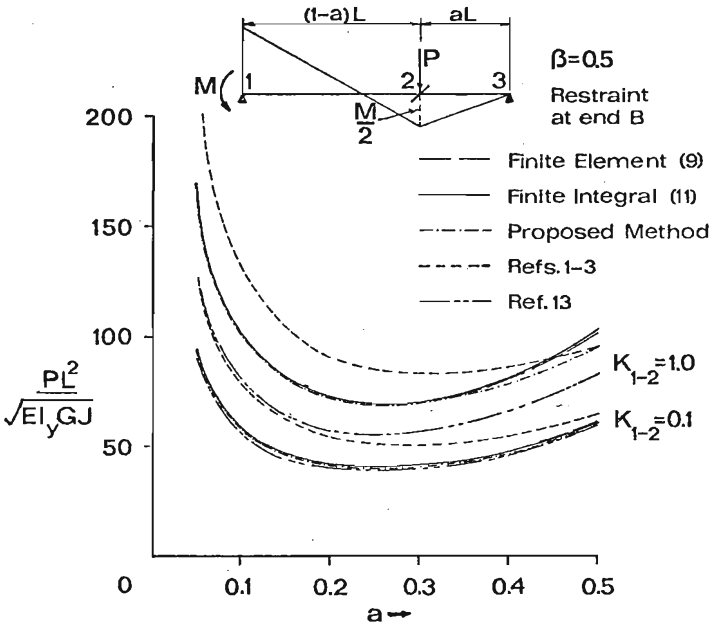

FIGURE 28(b) : Beam with point load and end moment

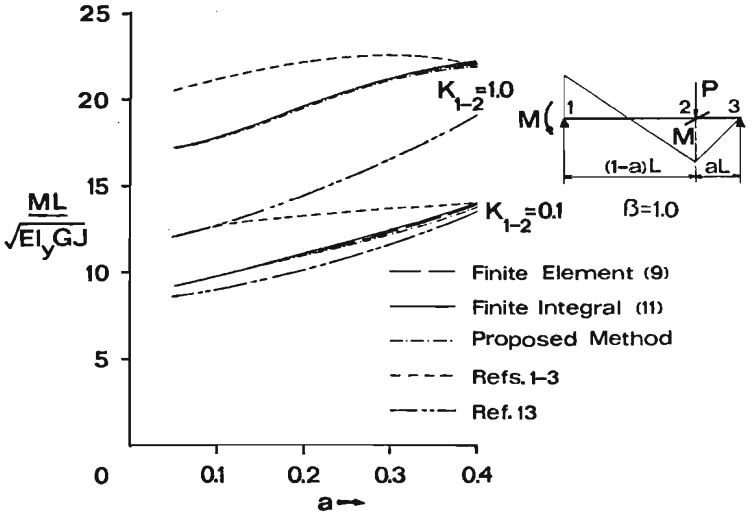

FIGURE 29 : Beam with point load and end moment

Generally the proposed method gives results which agree closely with those of the refined analyses (9,11). The authors have found this to hold for many other structures not presented in this paper. Salvadori's method (13) underestimates the buckling load, sometimes in a gross manner, except when no interaction occurs. The method of Nethercot and Trahair (1-3) tends to either overestimate or underestimate the buckling loads and this feature can be related directly to the effective length curves. By superimposing the curves for $\beta = -1.0$ over the other sets of curves, the likely regions of safe and unsafe predictions are clearly defined. As cycling reduces the estimated buckling load from that calculated in the first pass, its use is recommended with this method. However, there is no guarantee that unsafe estimates will be sufficiently reduced and furthermore, cycling will lower already conservative estimates.

8. CONCLUSIONS

An approximate method of determining the elastic critical loads of laterally continuous structures has been presented. The method which is based on the concept of effective length is a refinement of that proposed by Nethercot and Trahair (1-3). It can be applied to structures loaded at braced points at which lateral displacement and twisting are prevented.

A simple example of a three-segment laterally continuous beam of marrow rectangular cross-section shows that it is incorrect to equate the buckling load of a structure to that of one of its component parts or segments, without accounting for interaction between the parts. Basic principles involved in interaction buckling are explained. It is shown that the whole structure buckles in a single action. The approach to instability is followed in terms of individual segment behaviour modified by interaction. In this instance interaction involves a sharing of minor axis bending stiffness at the segment ends. It is shown that major axis loading causes a reduction in these stiffnesses. The structure responds more flexibly to a disturbing force set tending to produce minor axis end rotations which are characteristic of the buckling mode shape. As the major axis load increases one segment enters the negative end stiffness region but is restrained by the neighbouring segments which themselves are destabilised by this. Buckling occurs when this sharing of stiffness leaves the structure unable to resist even an infinitesmally small disturbing force set. A particular segment may have a pronounced effect on capacity by placing a high restraint demand and thus, a critical segment is defined along with a simple method to identify it.

In most I-beams, interaction at segment ends involves both minor axis bending and warping stiffnesses. A disturbing force set therefore has a moment and a bimoment at each segment end and it becomes impractical to attempt precise stability analyses by following segment stiffness variations and end interaction. The direct stiffness method of analysis as applied to more complex stability problems is then discussed. It is

noted that instability occurs when the stiffness matrix describing the relationship between disturbing forces and buckling displacements has a zero determinant.

It is proposed that a direct stiffness analysis of a substructure comprising the critical segment and its two adjacent segments gives an adequate estimation of the capacity of the entire structure. Appropriate boundary conditions are imposed at the ends of the adjacent segments. These segments offer restraint to the critical segment and parabolic approximations to determine the level of restraint available are developed. Load dependent end restraint parameters are added to the dimensionless exact stiffness matrix of the critical segment to complete the substructure stiffness matrix. The capacity of the structure is taken to equal that of the restrained critical segment.

Relationships between restraint parameters and buckling loads of restrained critical segments are presented as sets of critical segment effective length curves. The effective length, k, of a critical segment is shown to be a function of the restraint parameters, G_A and G_B; the moment gradient, β; and the critical segment beam parameter, K. Effective length charts are given for β in the range -1 to +1.0 and for K in the range 0.1 to 3.0. Inaccuracies in the commonly used expression for the moment modification factor, m, are compensated for in the charts.

A manual analysis procedure is outlined and examples of its use are given. The procedure involves cycling to ensure that the estimated buckling load is in close agreement with that used in the determination of the load dependent restraint parameters.

The method has been applied to a wide range of determinate and indeterminate beams and cantilevers and to simple beam grid systems. Some results are presented in the paper. In almost all cases it has predicted buckling loads to within a few percent of accurate numerical solutions.

9. ACKNOWLEDGEMENTS

The computer program used to plot the effective length curve data was written by Mr N.J. Richter and his assistance is gratefully acknowledged.

APPENDIX A - NOMENCLATURE

Symbol	Meaning
B_M	bimoment
B_{MA}, B_{MB}	applied bimoments at ends A and B respectively
$\overline{B}_{MA}, \overline{B}_{MB}$	non-dimensionalised bimoments (see Equation 10)
C	subscript referring to critical segment
E	Young's modulus of elasticity
f, f_1, f_2	stiffness coefficient
G	shear modulus of elasticity
G_A, G_B	restraint parameters (see Equation 14)
h	distance between flange shear centres
I_y	minor axis second moment of area
I_ω	warping section constant
J	torsion section constant
K	beam parameter = $\sqrt{\pi^2 EI_\omega / GJL^2}$, or stiffness matrix of structure
k	effective length factor
L	length of beam, or
L, L_S	length of beam segment
M	major axis moment
M_E	elastic critical moment
M_F	elastic critical moment of substructure
M_f	flange moment
M_y	minor axis moment
M_{yA}, M_{yB}	applied minor axis moments at ends A and B respectively
$\overline{M}_{yA}, \overline{M}_{yB}$	non-dimensional minor axis moments (see Equation 10)
m	moment modification factor
n	stiffness coefficient, commonly 2,3,4
R	subscript referring to restraining segment, or disturbing nodal force vector
r	nodal displacement vector
$S_{11}, .. S_{44}$	non-dimensional stiffness terms

Symbol	Meaning
u	out-of-plane deflection of shear centre
V_f	flange shear
x,y	major and minor principal axes
z	longitudinal axis
β	ratio of major axis end moments
γ	non-dimensionalised moment = $ML/\sqrt{EI_y GJ}$
γ_c	non-dimensionalised elastic critical moment of beam segment
γ_F	non-dimensionalised elastic critical moment of substructure
θ_y	minor axis end rotation
θ_{yA}, θ_{yB}	minor axis end rotations at ends A and B respectively
$\bar{\theta}_{yA}, \bar{\theta}_{yB}$	non-dimensionalised minor axis end rotations (see Equation 10)
λ	load factor
λ_C	load factor referred to critical segment
λ_F	load factor of substructure
λ_R	load factor referred to restraining segment
ϕ	angle of twist
ϕ'	first derivative of ϕ with respect to coordinate z
ϕ'_A, ϕ'_B	first derivatives at ends A and B respectively
$\bar{\phi}'_A, \bar{\phi}'_B$	non-dimensionalised first derivatives (see Equation 10)

APPENDIX B - REFERENCES

1. NETHERCOT, D.A. and TRAHAIR, N.S., "Lateral Buckling Approximations for Elastic Beams", *The Structural Engineer*, Vol. 54, No. 6, 1976, pp. 197-204.

2. NETHERCOT, D.A. and TRAHAIR, N.S., "Inelastic Lateral Buckling of Determinate Beams", *Journal of the Structural Division*, ASCE, Vol. 102, No. ST4, April 1976, pp. 701-717.

3. NETHERCOT, D.A. and TRAHAIR, N.S., "Lateral Buckling Calculations for Braced Beams", *Civil Engineering Transactions*, Institution of Engineers, Australia, Vol. CE19, No. 2, 1977, p. 211.

4. KITIPORNCHAI, S. and DUX, P.F., Discussion of "Lateral Buckling of Intersecting Connected Beams", *Journal of the Engineering Mechanics Division*, ASCE, Vol. 105, No. EM3, June 1979, pp. 490-492.

5. AMERICAN INSTITUTE OF STEEL CONSTRUCTION, "Specification for the Design, Fabrication and Erection of Structural Steel for Buildings", AISC, New York, 1969.

6. BRITISH STANDARDS INSTITUTION, "BS 449:1969 Specification for the Use of Structural Steel in Buildings", BSI, London.

7. STANDARDS ASSOCIATION OF AUSTRALIA, "AS 1250-1975 SAA Steel Structures Code", SAA, Sydney, 1975.

8. POWELL, G. and KLINGNER, R., "Elastic Lateral Buckling of Steel Beams", *Journal of the Structural Division*, ASCE, Vol. 96, No. ST9, September 1970, p. 1919.

9. CONNOR, T.B., "Elastic and Elasto-Plastic Beam Buckling Using Finite Element Methods", *Ph.D. Thesis*, University of Queensland, 1974.

10. KITIPORNCHAI, S., "Stability of Steel Structures", *Ph.D. Thesis*, University of Sydney, 1973.

11. RICHTER, N.J., "Application of the Finite Integral Method to Lateral Buckling of Beams", *M.Eng.Sc. Thesis*, University of Queensland, 1979.

12. TRAHAIR, N.S., *The Behaviour and Design of Steel Structures*, Chapman and Hall, London, 1977.

13. SALVADORI, M.G., "Lateral Buckling of Beams of Rectangular Cross-Section Under Bending and Shear", *Proceedings*, 1st U.S. National Congress of Applied Mechanics, 1951, p.403.

14. KIPIPORNCHAI, S. and RICHTER, N.J., "Elastic Lateral Buckling of Beams with Discrete Intermediate Restraints", *Civil Engineering Transactions*, Institution of Engineers, Australia, Vol. CE20, No. 2, 1978, pp. 105-111.

15. HORNE, M.R. and MERCHANT, W., *The Stability of Frames*, Pergamon Press, New York, 1965.

16. DUX, P.F. "Elastic and Inelastic Buckling of Laterally Continuous Structures", *Ph.D. Thesis*, University of Queensland, in preparation.

17. VLASOV, V.Z., *Thin Walled Elastic Beams*, 2nd ed., Israel Program for Scientific Translations, Jerusalem, Israel, 1961.

18. SOKOLNIKOFF, I.S. and REDHEFFER, R.M., *Mathematics of Physics and Modern Engineering*, McGraw-Hill Book Co., New York, 1958.

19. TRAHAIR, N.S., "Stability of I-beams with Elastic End Restraints", *Journal of the Institution of Engineers, Australia*, Vol. 37, No. 6, June 1965, pp. 157-168.

CIVIL ENGINEERING RESEARCH REPORTS

CE No.	Title	Author(s)	Date
1	Flood Frequency Analysis: Logistic Method for Incorporating Probable Maximum Flood	BRADY, D.K.	February, 1979
2	Adjustment of Phreatic Line in Seepage Analysis by Finite Element Method	ISAACS, L.T.	March, 1979
3	Creep Buckling of Reinforced Concrete Columns	BEHAN, J.E. & O'CONNOR, C.	April, 1979
4	Buckling Properties of Monosymmetric I-Beams	KITIPORNCHAI, S. & TRAHAIR, N.S.	May, 1979
5	Elasto-Plastic Analysis of Cable Net Structures	MEEK, J.L. & BROWN, P.L.D.	November, 1979
6	A Critical State Soil Model for Cyclic Loading	CARTER, J.P., BOOKER, J.R. & WROTH, C.P.	December, 1979
7	Resistance to Flow in Irregular Channels	KAZEMIPOUR, A.K. & APELT, C.J.	February, 1980
8	An Appraisal of the Ontario Equivalent Base Length	O'CONNOR, C.	February, 1980
9	Shape Effects on Resistance to Flow in Smooth Rectangular Channels	KAZEMIPOUR, A.K. & APELT, C.J.	April, 1980
10	The Analysis of Thermal Stress Involving Non-Linear Material Behaviour	BEER, G. & MEEK, J.L.	April, 1980
11	Buckling Approximations for Laterally Continuous Elastic I-Beams	DUX, P.F. & KITIPORNCHAI, S.	April, 1980
12	A Second Generation Frontal Solution Program	BEER, G.	May, 1980
13	Combined Stiffness for Beam and Column Braces	O'CONNOR, C.	May, 1980
14	Beaches:- Profiles, Processes and Permeability	GOURLAY, M.R.	June, 1980

CURRENT CIVIL ENGINEERING BULLETINS

4 *Brittle Fracture of Steel — Performance of ND1B and SAA A1 structural steels: C. O'Connor (1964)*

5 *Buckling in Steel Structures — 1. The use of a characteristic imperfect shape and its application to the buckling of an isolated column: C. O'Connor (1965)*

6 *Buckling in Steel Structures — 2. The use of a characteristic imperfect shape in the design of determinate plane trusses against buckling in their plane: C. O'Connor (1965)*

7 *Wave Generated Currents — Some observations made in fixed bed hydraulic models: M.R. Gourlay (1965)*

8 *Brittle Fracture of Steel — 2. Theoretical stress distributions in a partially yielded, non-uniform, polycrystalline material: C. O'Connor (1966)*

9 *Analysis by Computer — Programmes for frame and grid structures: J.L. Meek (1967)*

10 *Force Analysis of Fixed Support Rigid Frames: J.L. Meek and R. Owen (1968)*

11 *Analysis by Computer — Axisymetric solution of elasto-plastic problems by finite element methods: J.L. Meek and G. Carey (1969)*

12 *Ground Water Hydrology: J.R. Watkins (1969)*

13 *Land use prediction in transportation planning: S. Golding and K.B. Davidson (1969)*

14 *Finite Element Methods — Two dimensional seepage with a free surface: L.T. Isaacs (1971)*

15 *Transportation Gravity Models: A.T.C. Philbrick (1971)*

16 *Wave Climate at Moffat Beach: M.R. Gourlay (1973)*

17. *Quantitative Evaluation of Traffic Assignment Methods: C. Lucas and K.B. Davidson (1974)*

18 *Planning and Evaluation of a High Speed Brisbane-Gold Coast Rail Link: K.B. Davidson, et al. (1974)*

19 *Brisbane Airport Development Floodway Studies: C.J. Apelt (1977)*

20 *Numbers of Engineering Graduates in Queensland: C. O'Connor (1977)*